The Satellite Auroral Footprints at Jupiter: A Juno Perspective

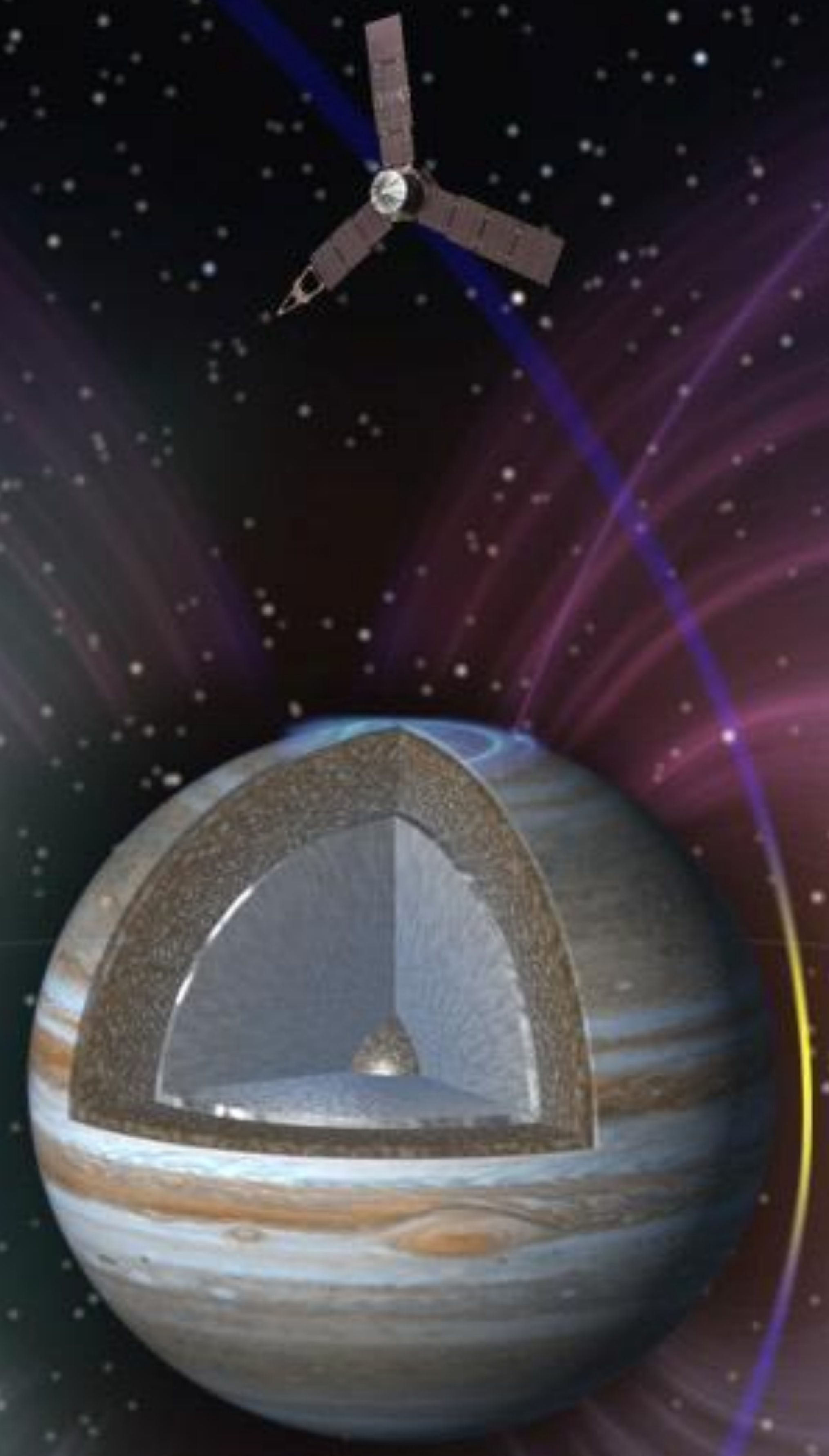

Vincent Hue

Aix-Marseille University
Institut Origines
Laboratoire d’Astrophysique de Marseille
http://vincenthue.com

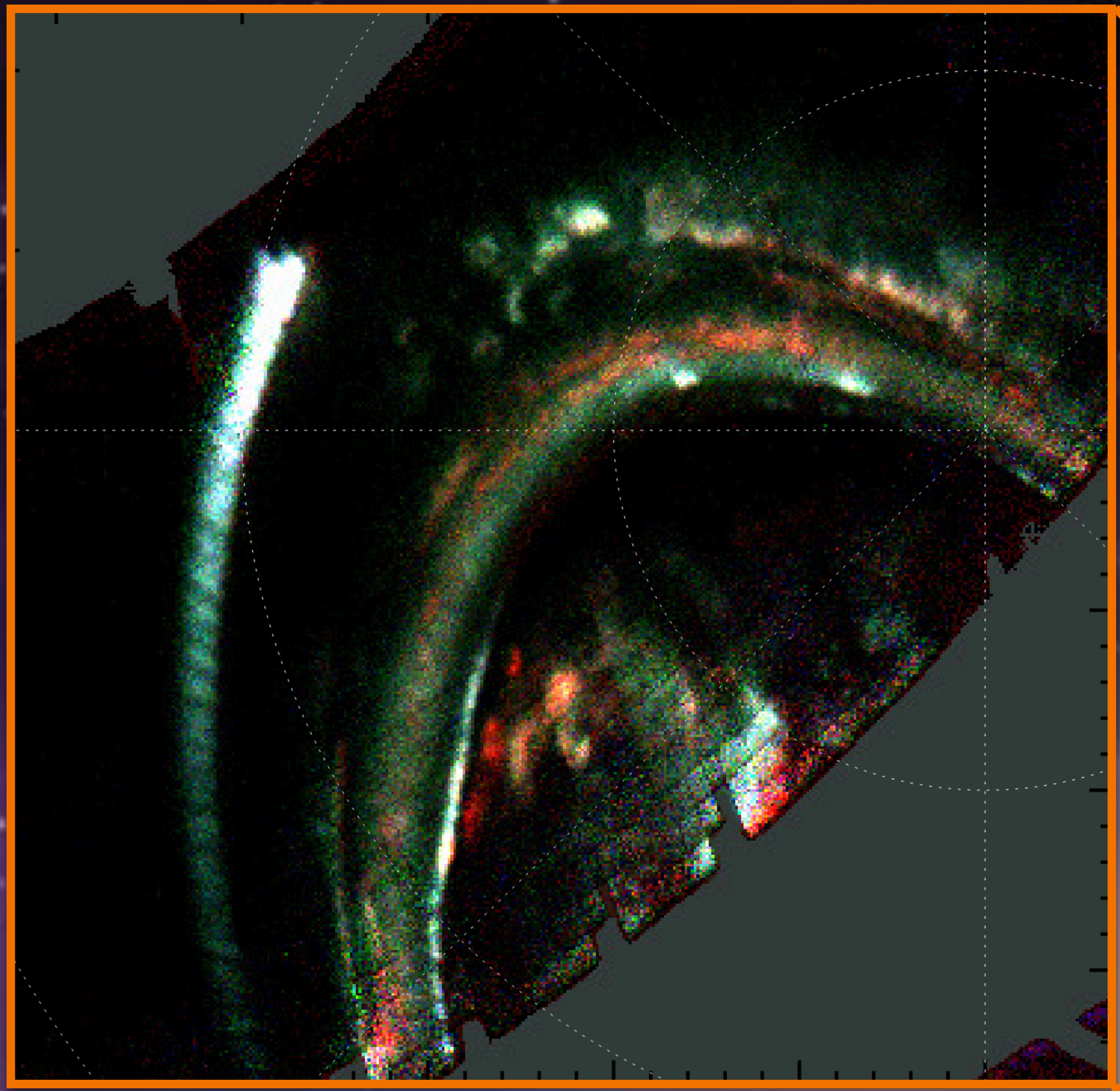

The Satellite Auroral Footprints at Jupiter: A Juno Perspective

Vincent Hue

Aix-Marseille University
Institut Origines
Laboratoire d’Astrophysique de Marseille
http://vincenthue.com

The Satellite Auroral Footprints at Jupiter

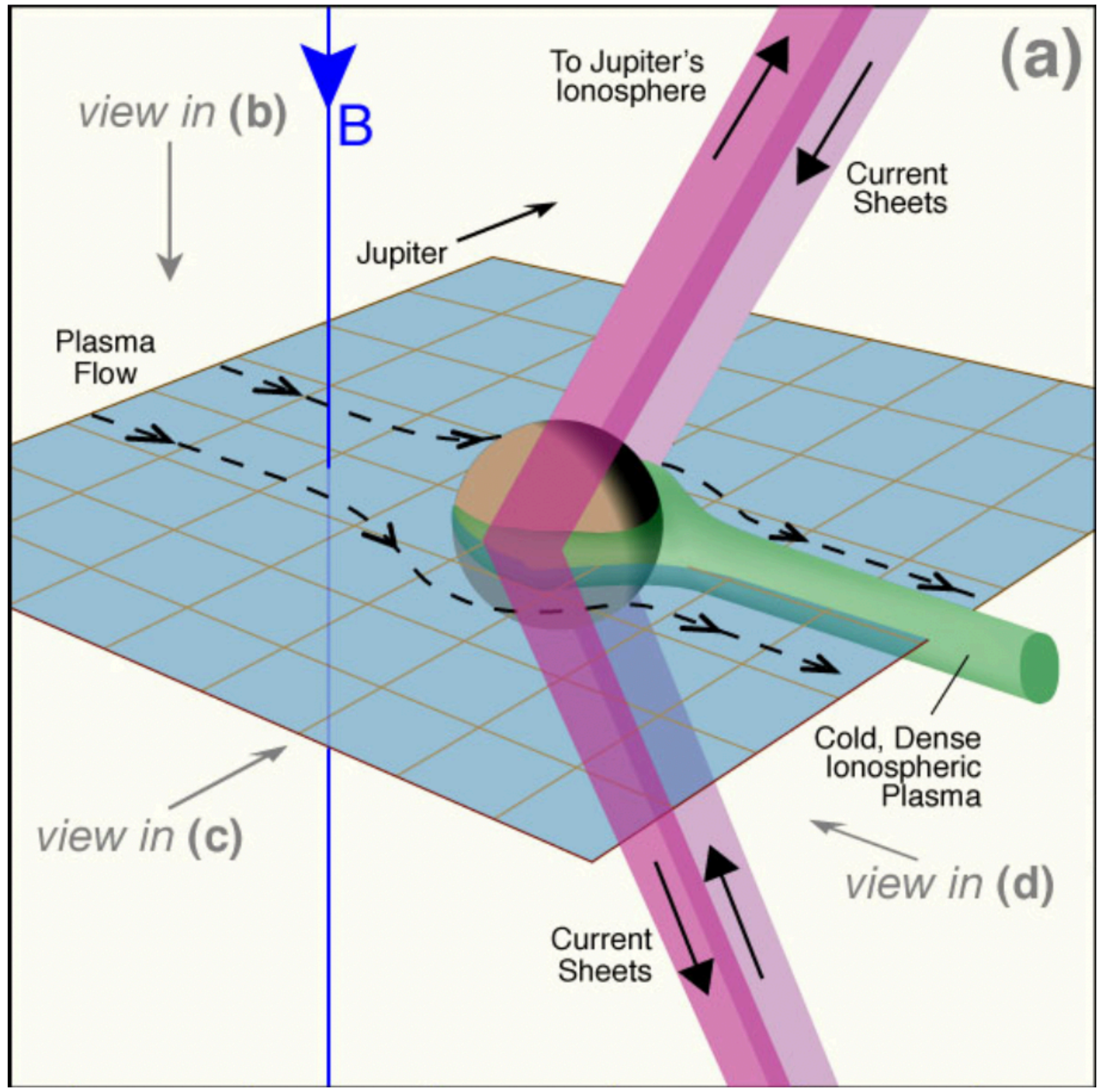

Bagenal 2007

The Satellite Auroral Footprints at Jupiter

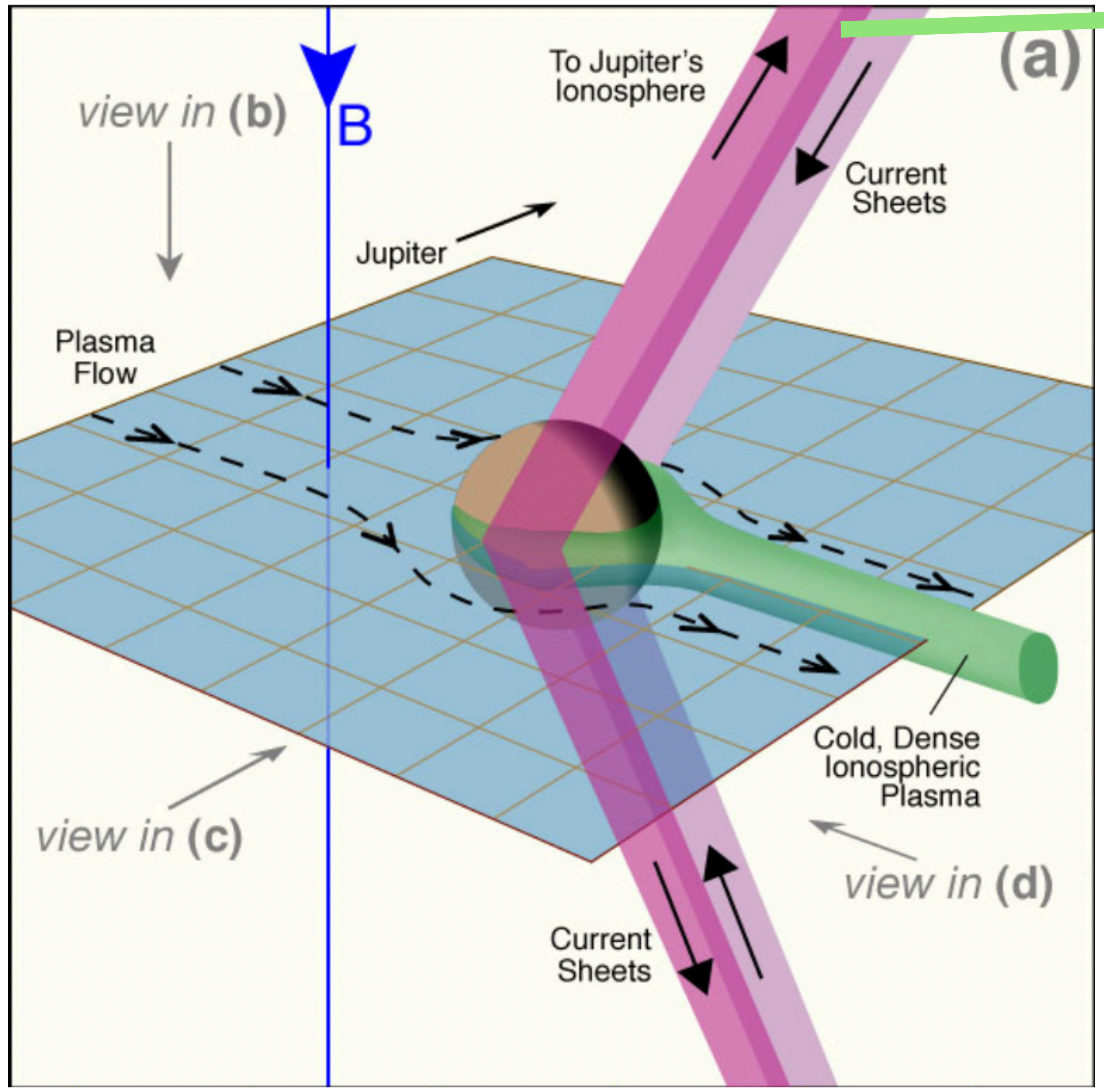

Bagenal 2007

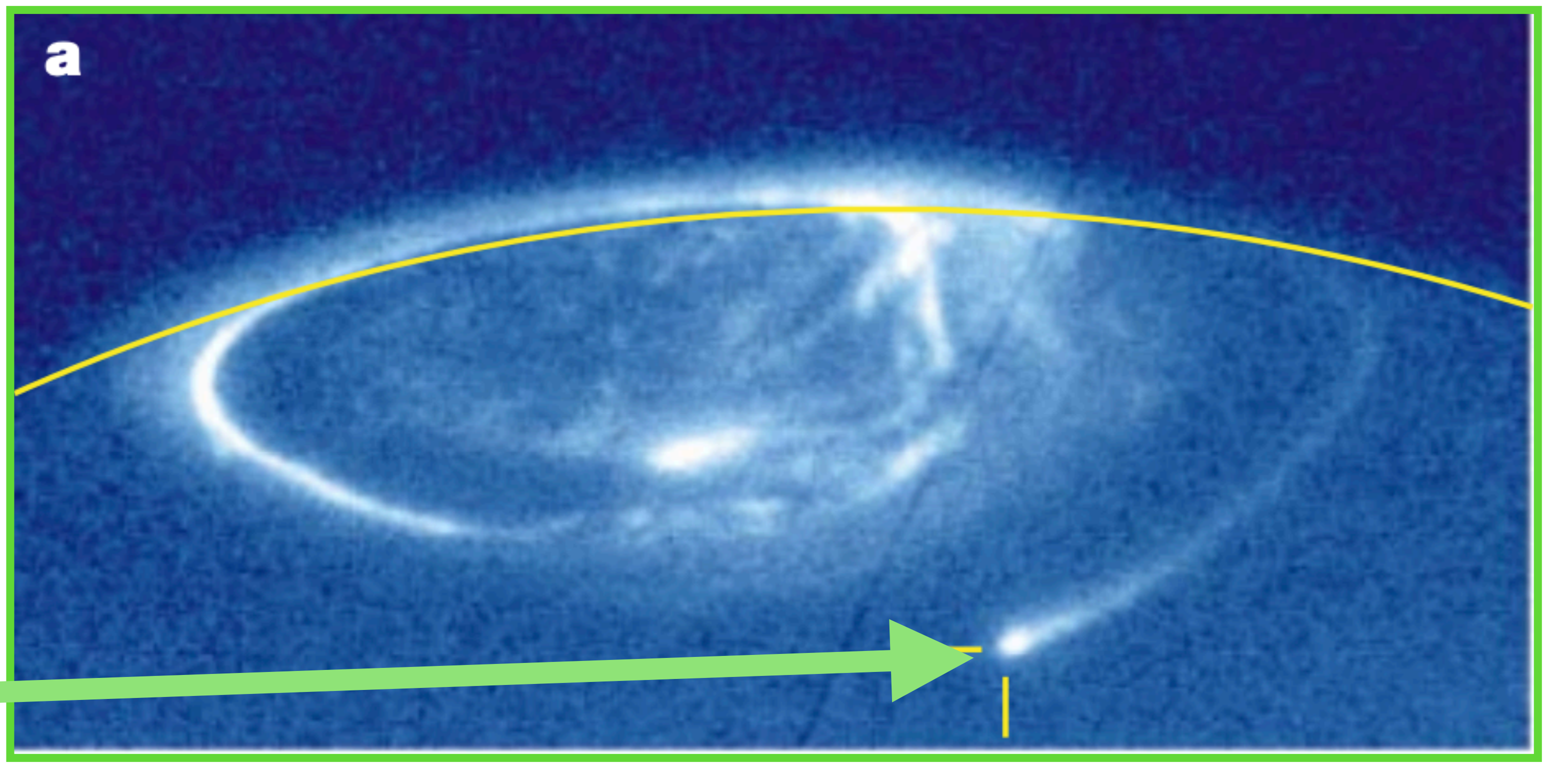

The Satellite Auroral Footprints at Jupiter

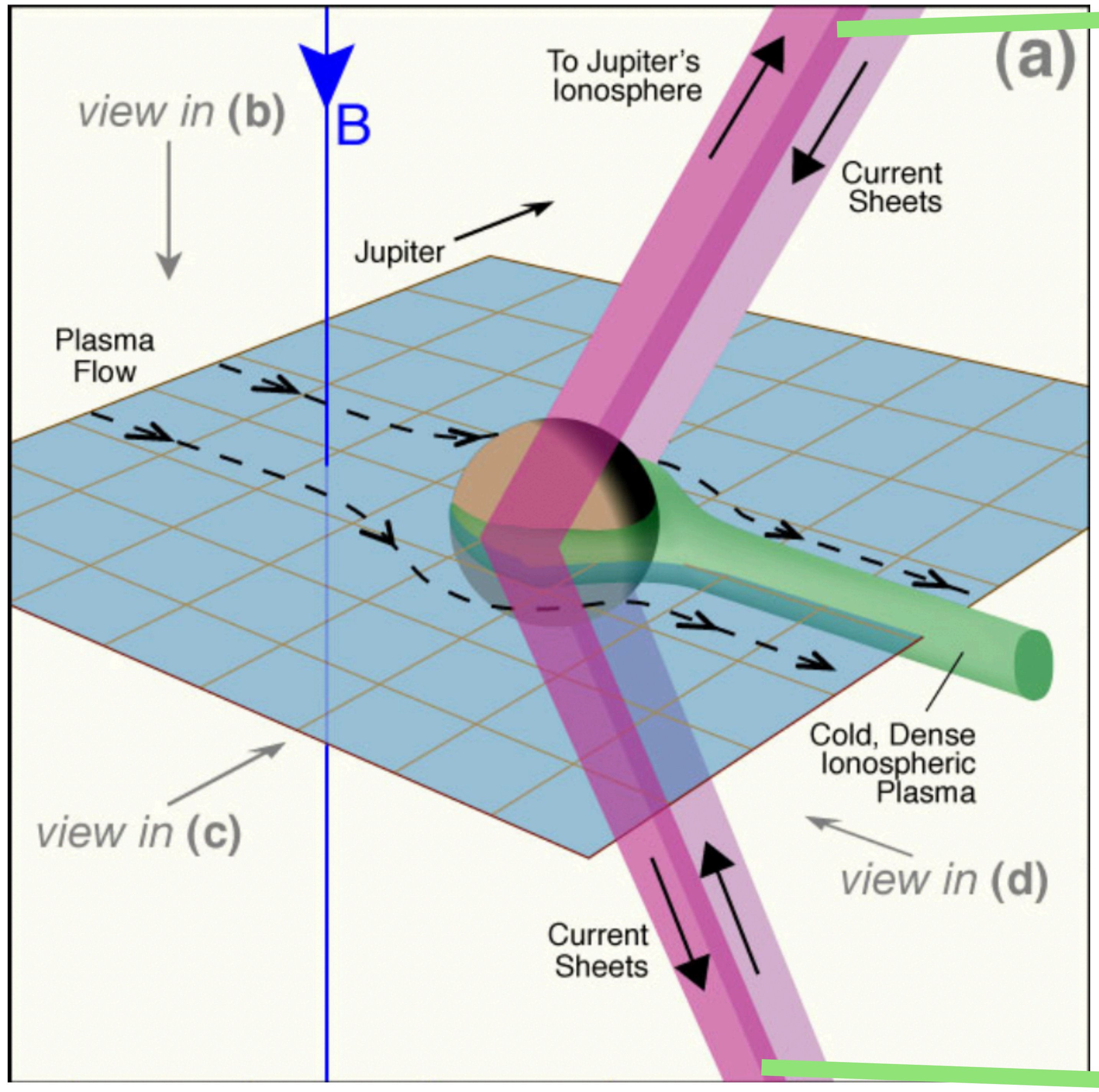

Bagenal 2007

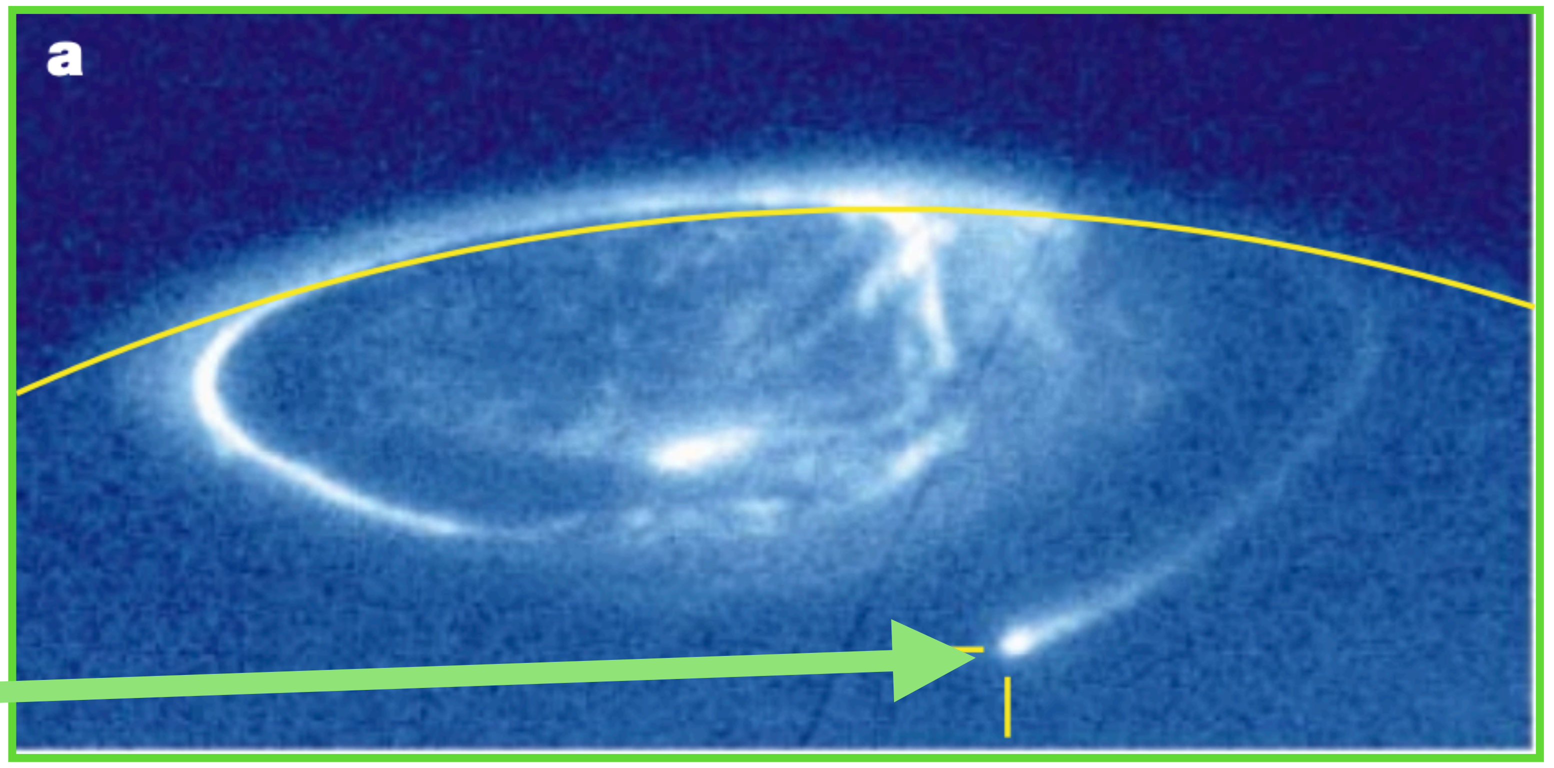

Clarke+2002

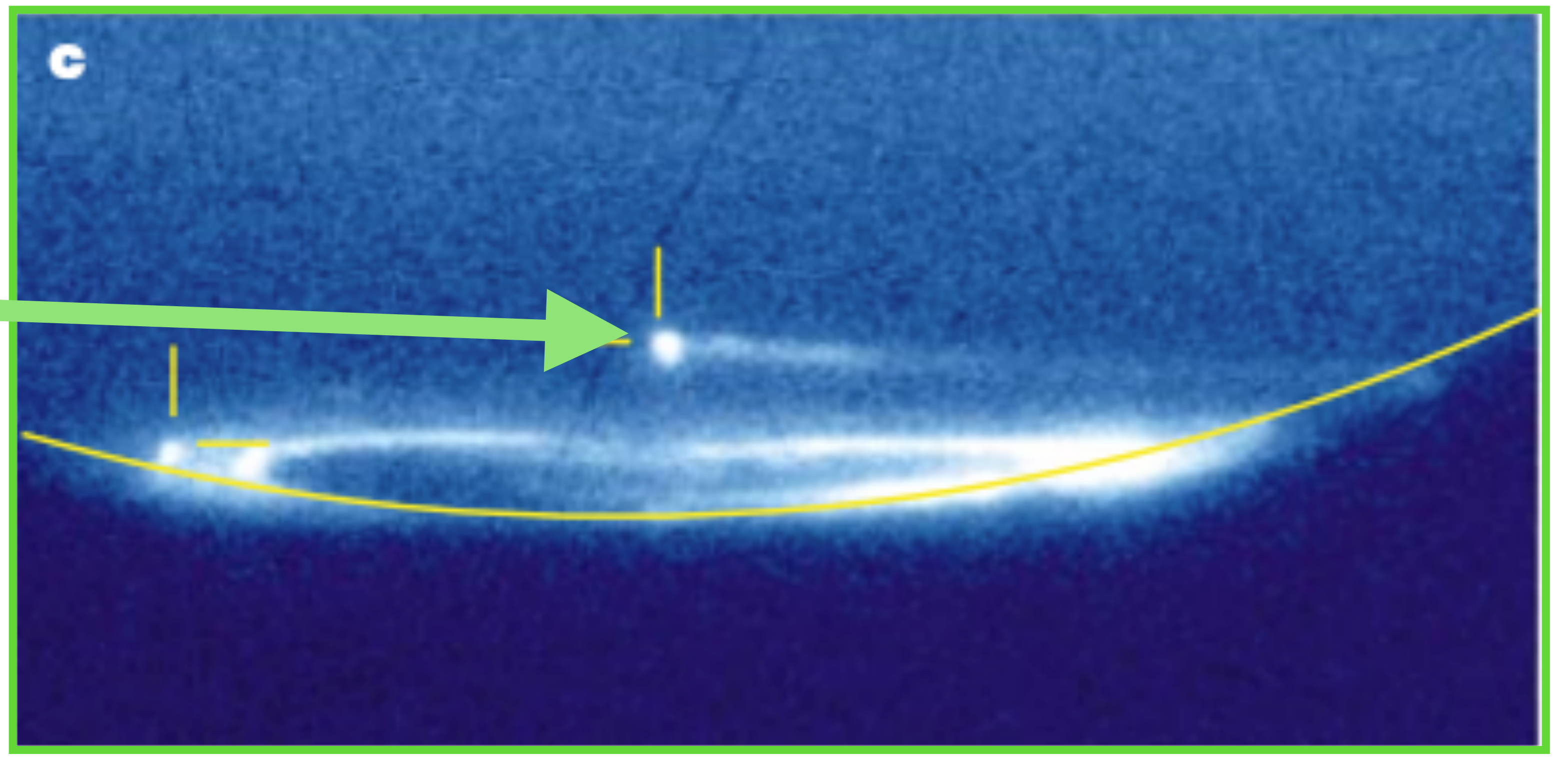

Two mechanisms to explain the tail emission

Quasi-steady current system

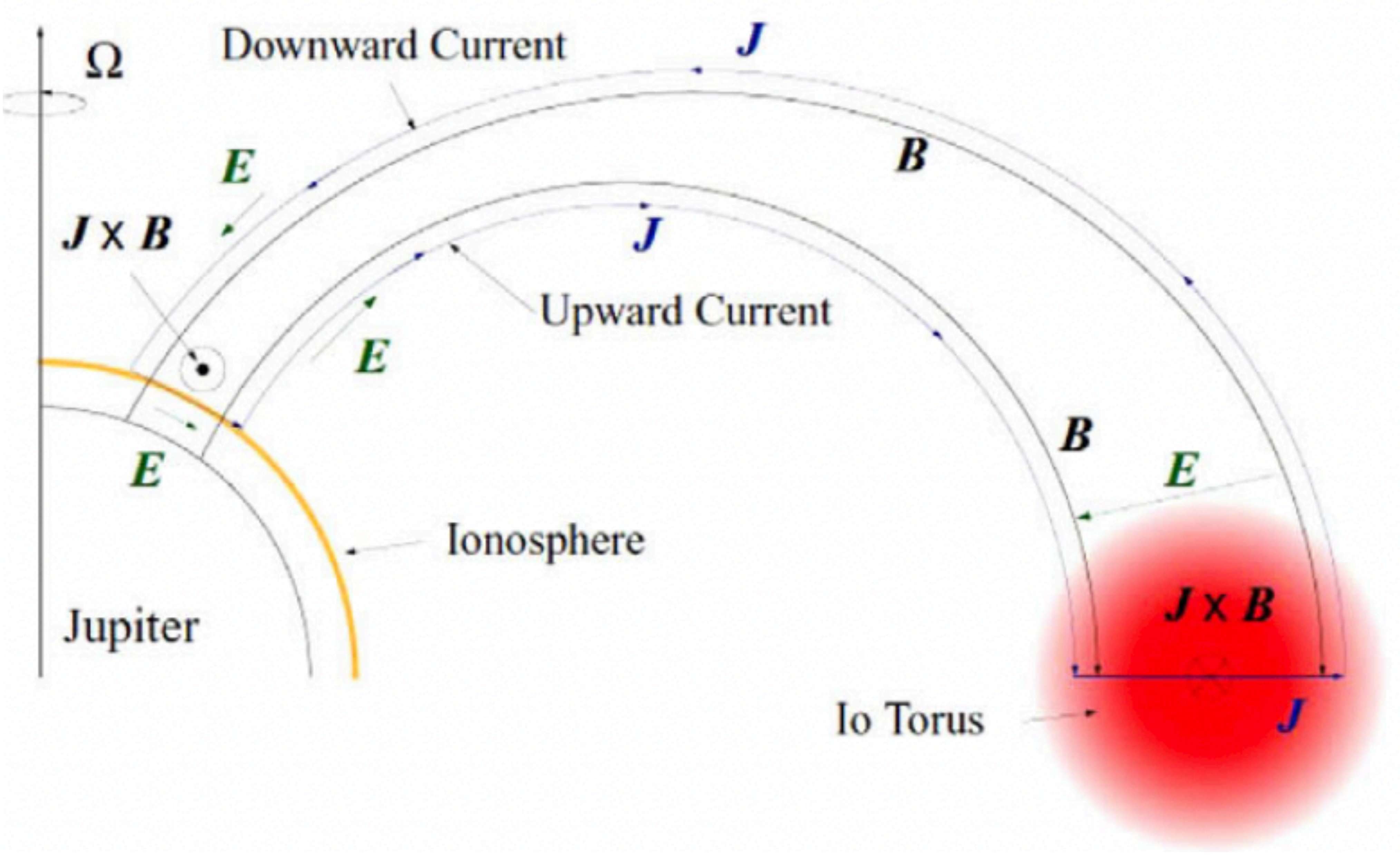

Birkeland current systems between Io's wake and Jupiter
Transfer of angular momentum from Jupiter's ionosphere to the plasma wake
➡ Peaked electron intensities in the tens keV range

e.g., Hill & Vasiliunas 2002; Delamere+2003; Su+2003; Ergun+2009

Multiple Alfvén waves reflections

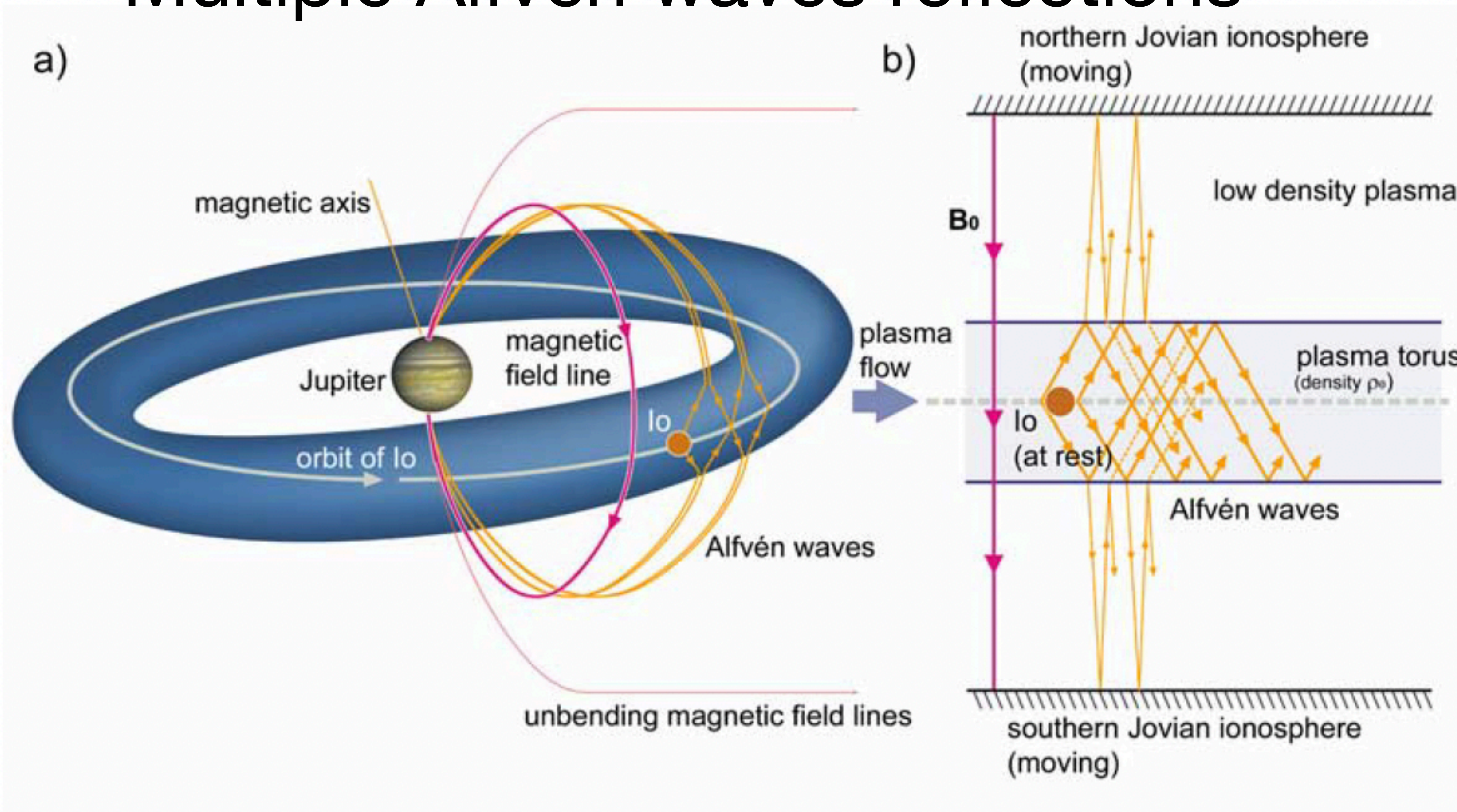

Multiple reflection of Alfvén waves in Io's wake
➡Broadband electron energy distribution downtail

e.g., Crary & Bagenal 1997; Jacobsen+2007 ; Hess+2010; Bonfond+2017; Szalay+2020

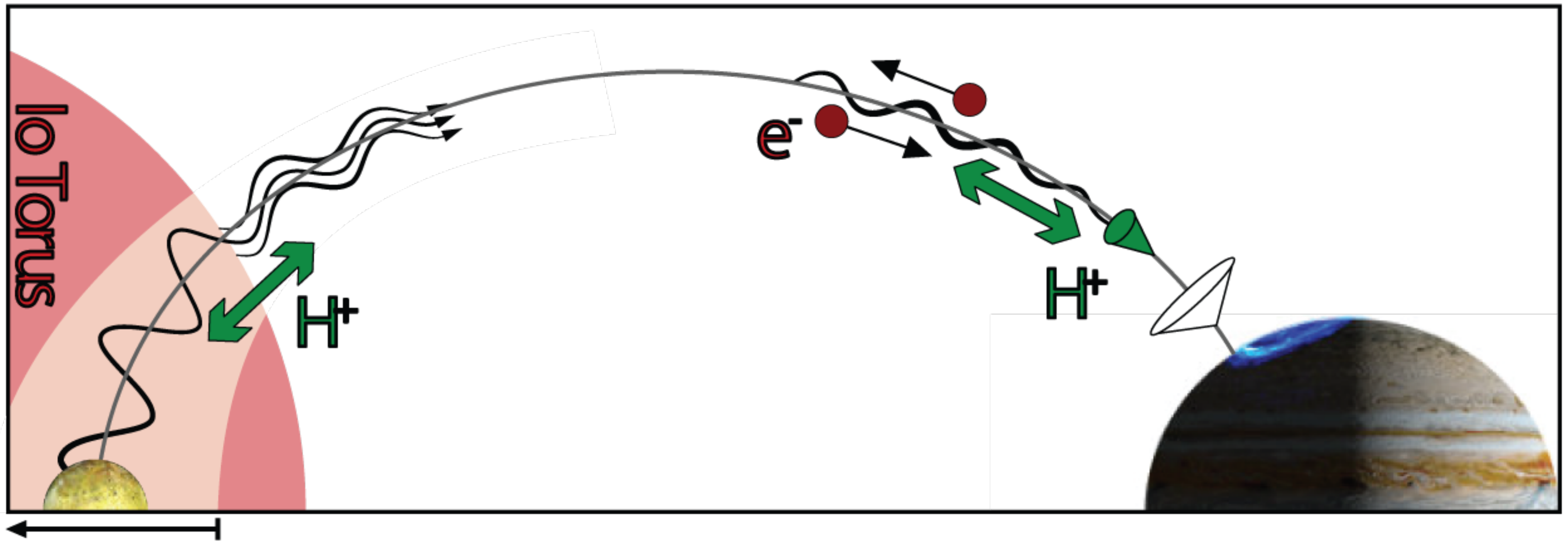

Courtesy:
J. R. Szalay

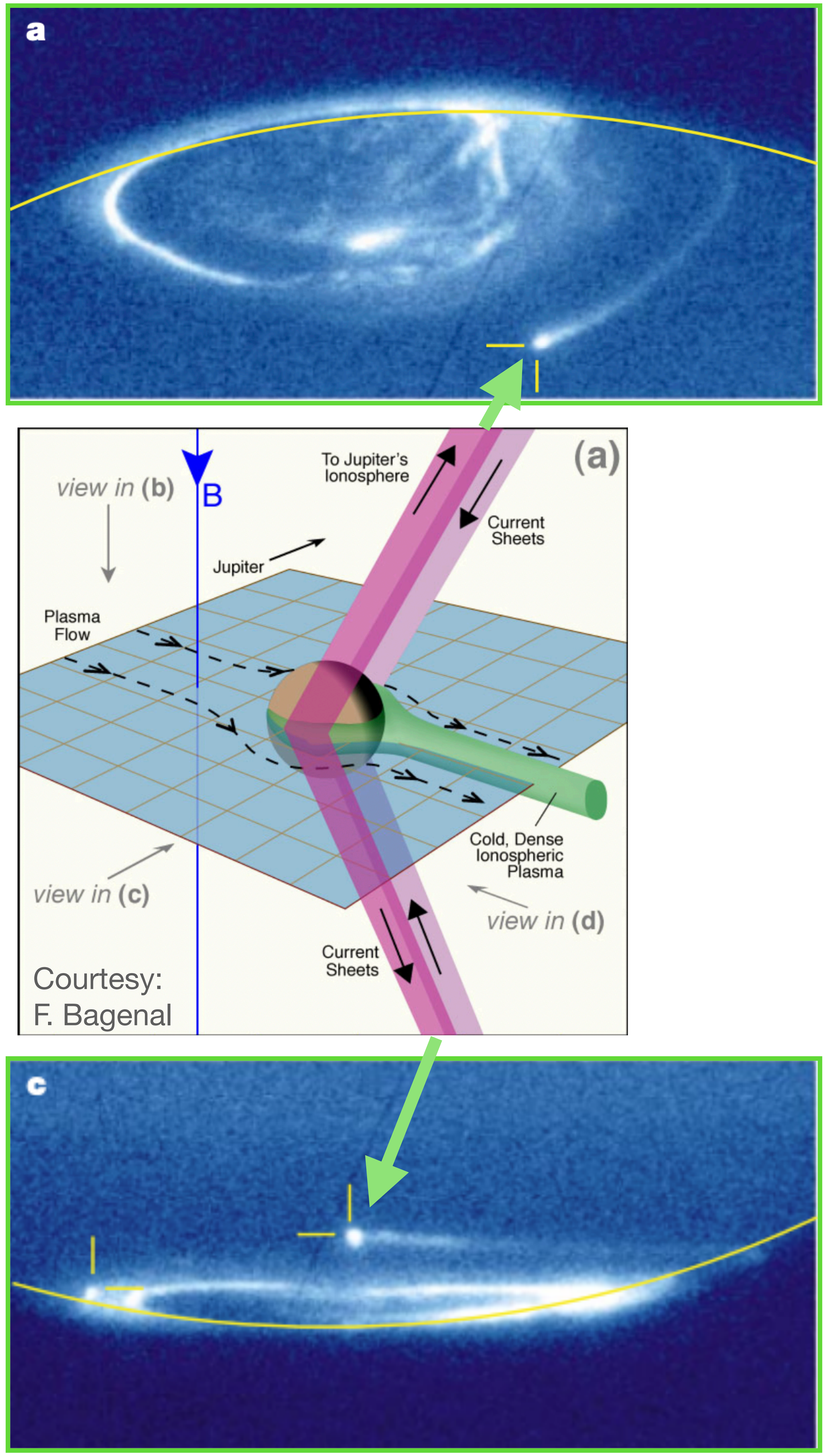

Courtesy:
F. Bagenal

Ground truth from Juno

- All crossings exhibit broad, power law-like intensity distributions
- Suggests Alfvénic acceleration sustaining tail emissions

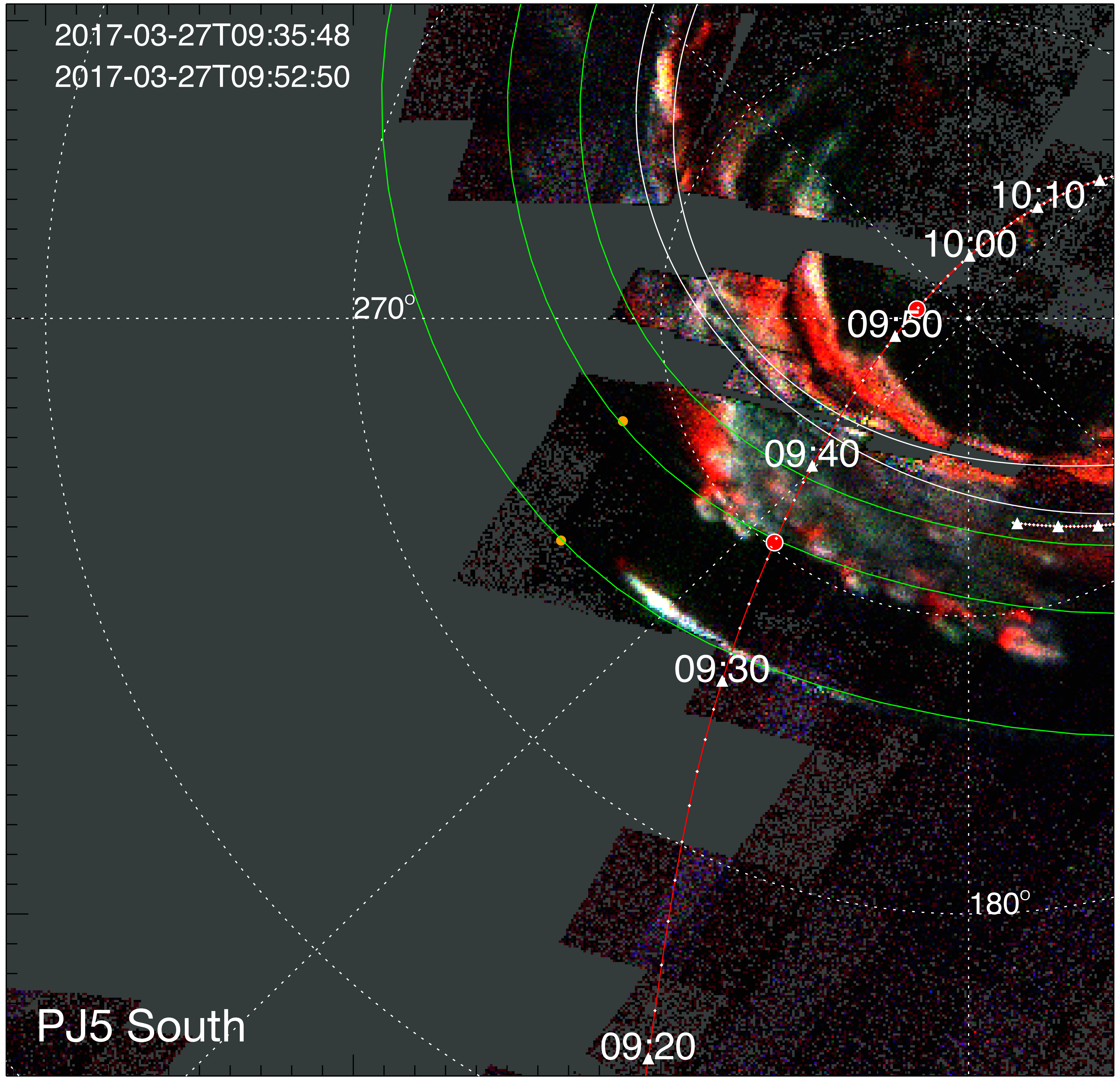

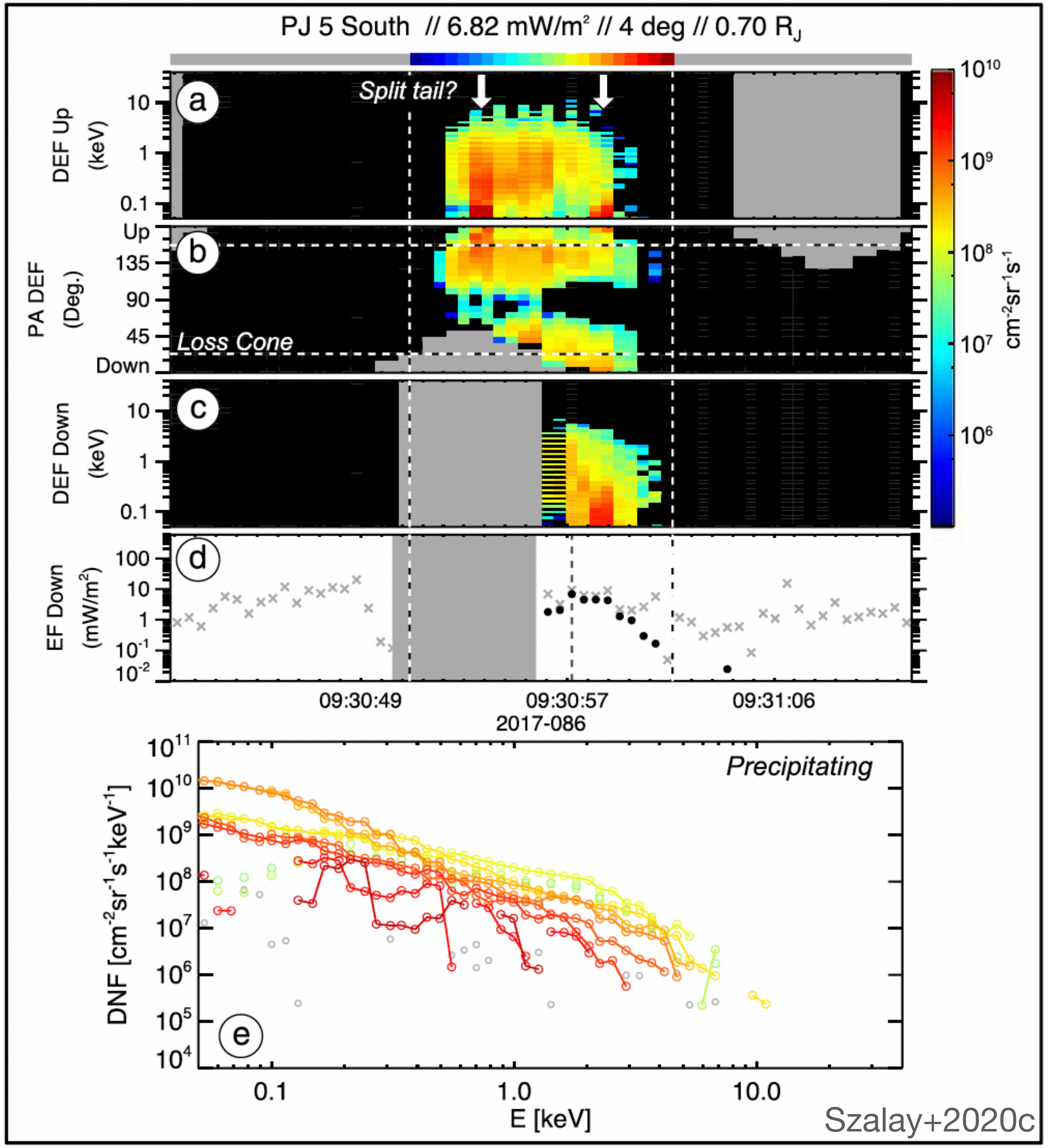

Szalay+2020c

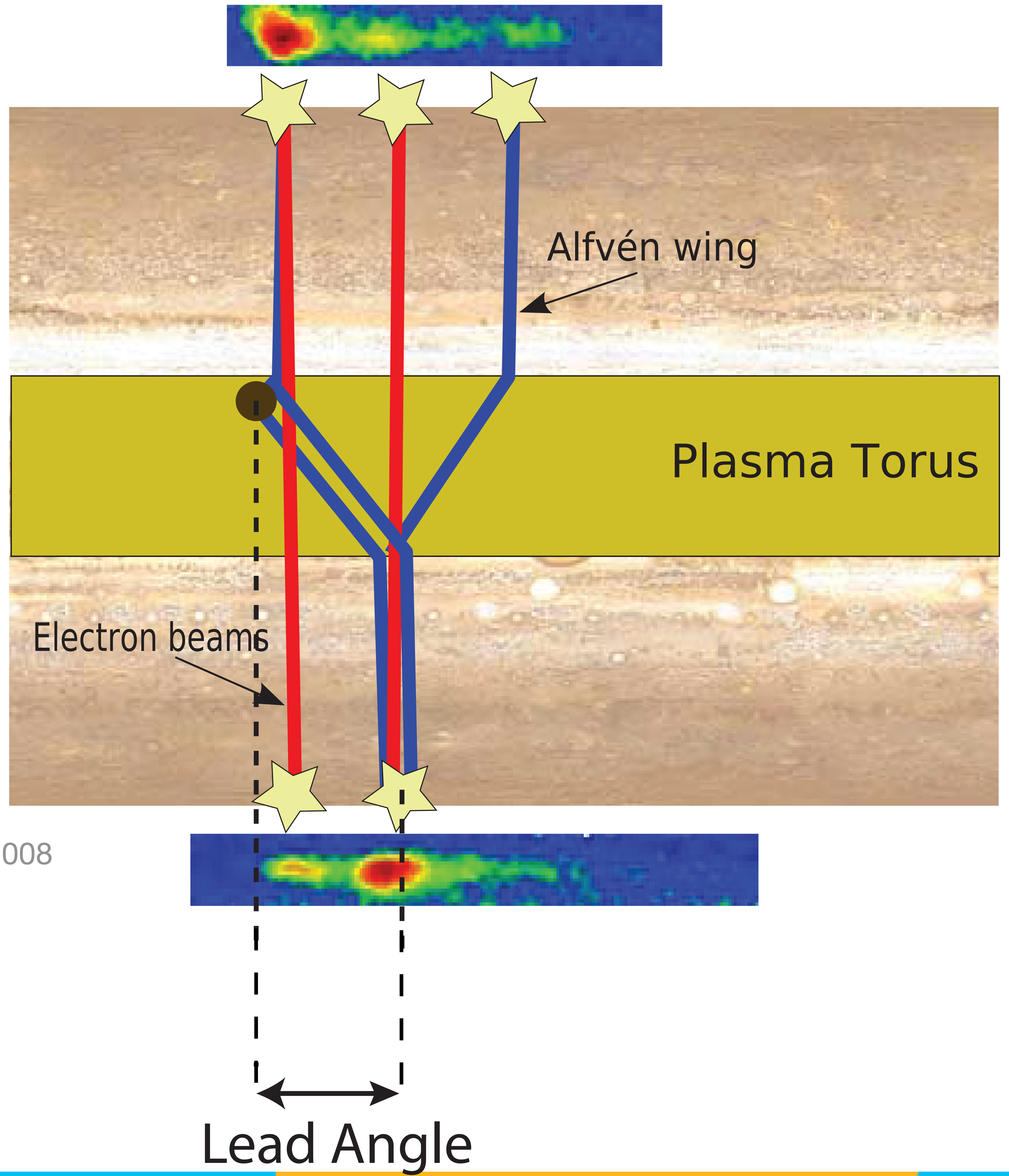

Bonfond+2008

- Brightness & morphology of footprints controlled by the position of the satellite within the plasma sheet
  (Gérard+ 2006; Bonfond+ 2008, 2009, 2013; Hess+ 2010, 2013)

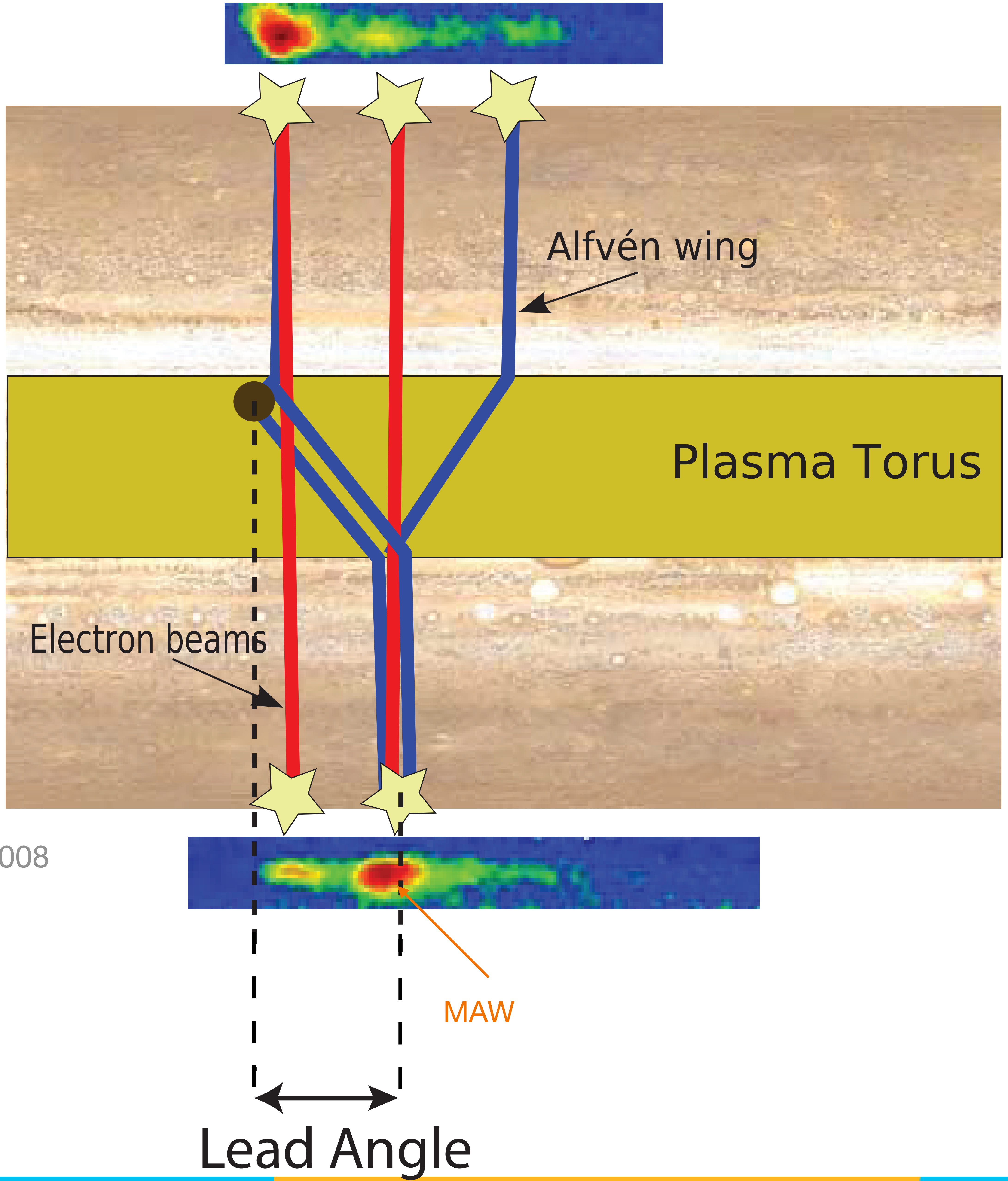

Bonfond+2008

- Brightness & morphology of footprints controlled by the position of the satellite within the plasma sheet
  (Gérard+ 2006; Bonfond+ 2008, 2009, 2013; Hess+ 2010, 2013)

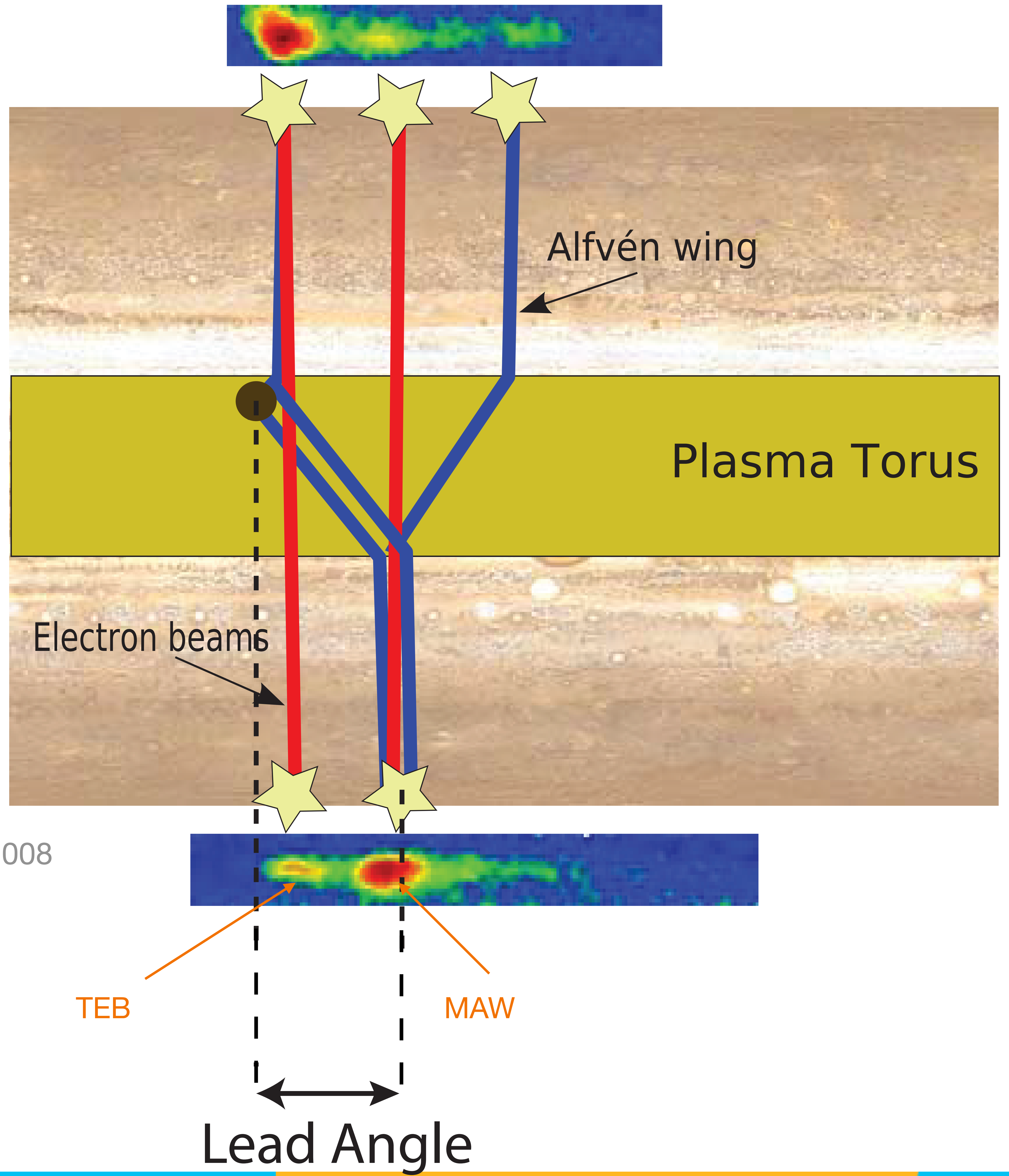

Bonfond+2008

- Brightness & morphology of footprints controlled by the position of the satellite within the plasma sheet
  (Gérard+ 2006; Bonfond+ 2008, 2009, 2013; Hess+ 2010, 2013)

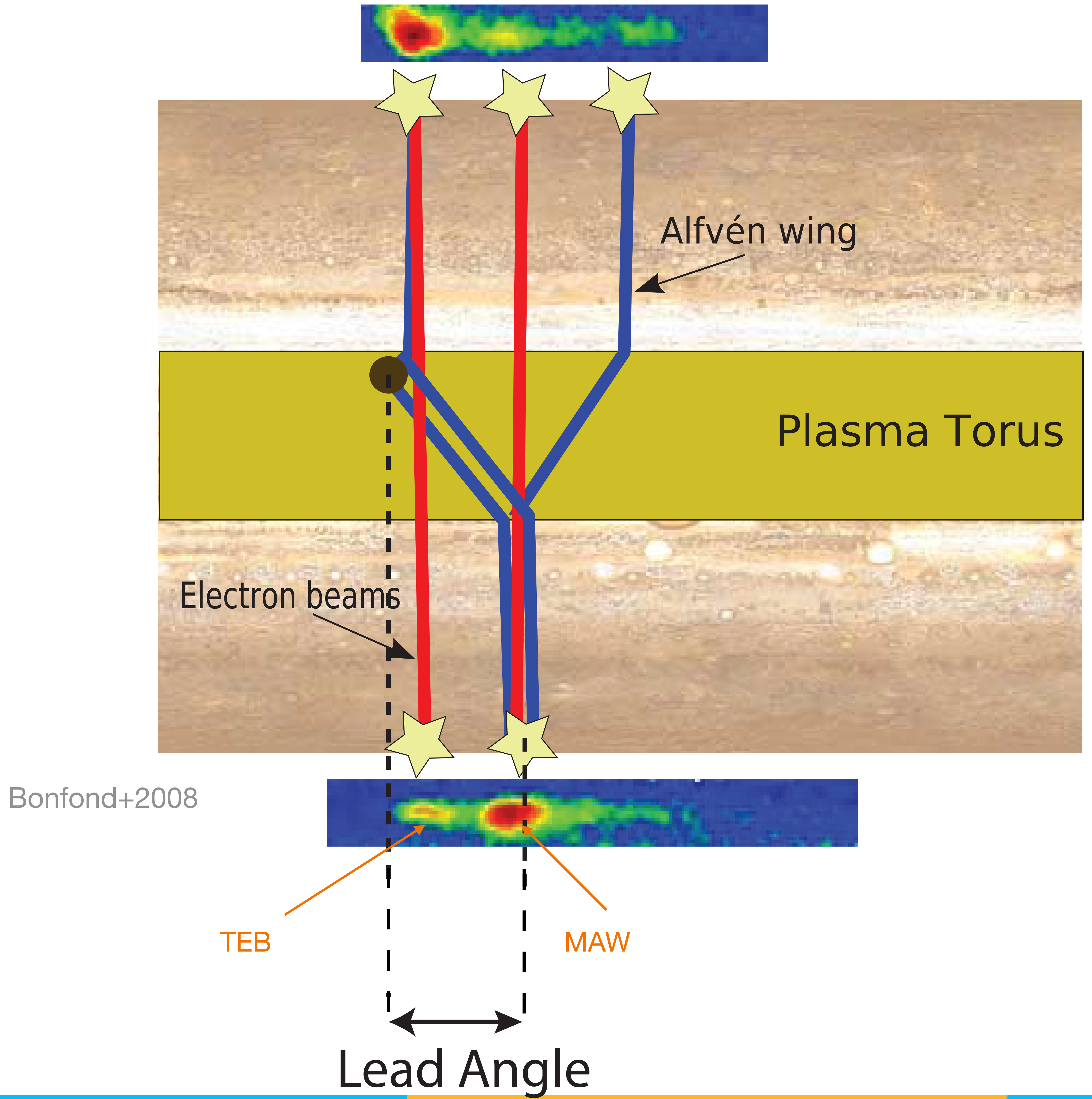

- Brightness & morphology of footprints controlled by the position of the satellite within the plasma sheet (Gérard+ 2006; Bonfond+ 2008, 2009, 2013; Hess+ 2010, 2013)

- Allows to better order the Juno satellite flux tube crossing in-situ measurements (Szalay+2020; Rabia+2023)

- Controls the timing of the satellite induced radio emission (Hess+2010)

- Provide indirect information about the plasma and magnetic conditions (Hinton+2018; Moirano+2023; Schlegel+2023)

Satellite footprint family portait from Juno-UVS

- **Lead angle**: Shift between the magnetic mapping and Alfvénic mapping of the moon

- 1600 individual spectral images exploited of the Io, Europa, and Ganymede footprints (PJ1 - PJ43)

- Map the lead angle in the equatorial plane using JRM33 + CON2020 models (Connerney+ 2020, 2121)

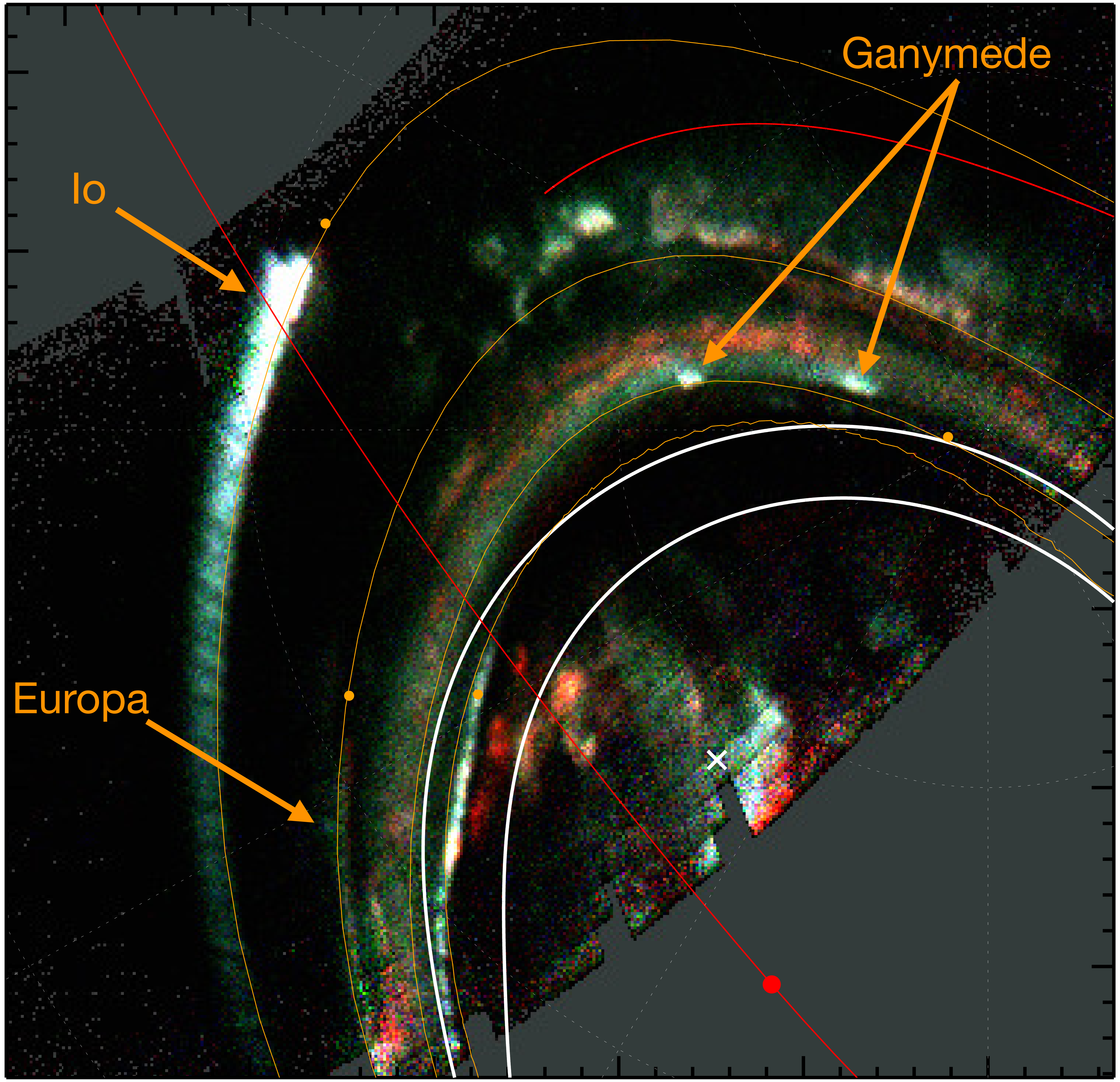

Satellite footprint family portait from Juno-UVS

- **Lead angle**: Shift between the magnetic mapping and Alfvénic mapping of the moon
- 1600 individual spectral images exploited of the Io, Europa, and Ganymede footprints (PJ1 - PJ43)
- Map the lead angle in the equatorial plane using JRM33 + CON2020 models (Connerney+ 2020, 2121)

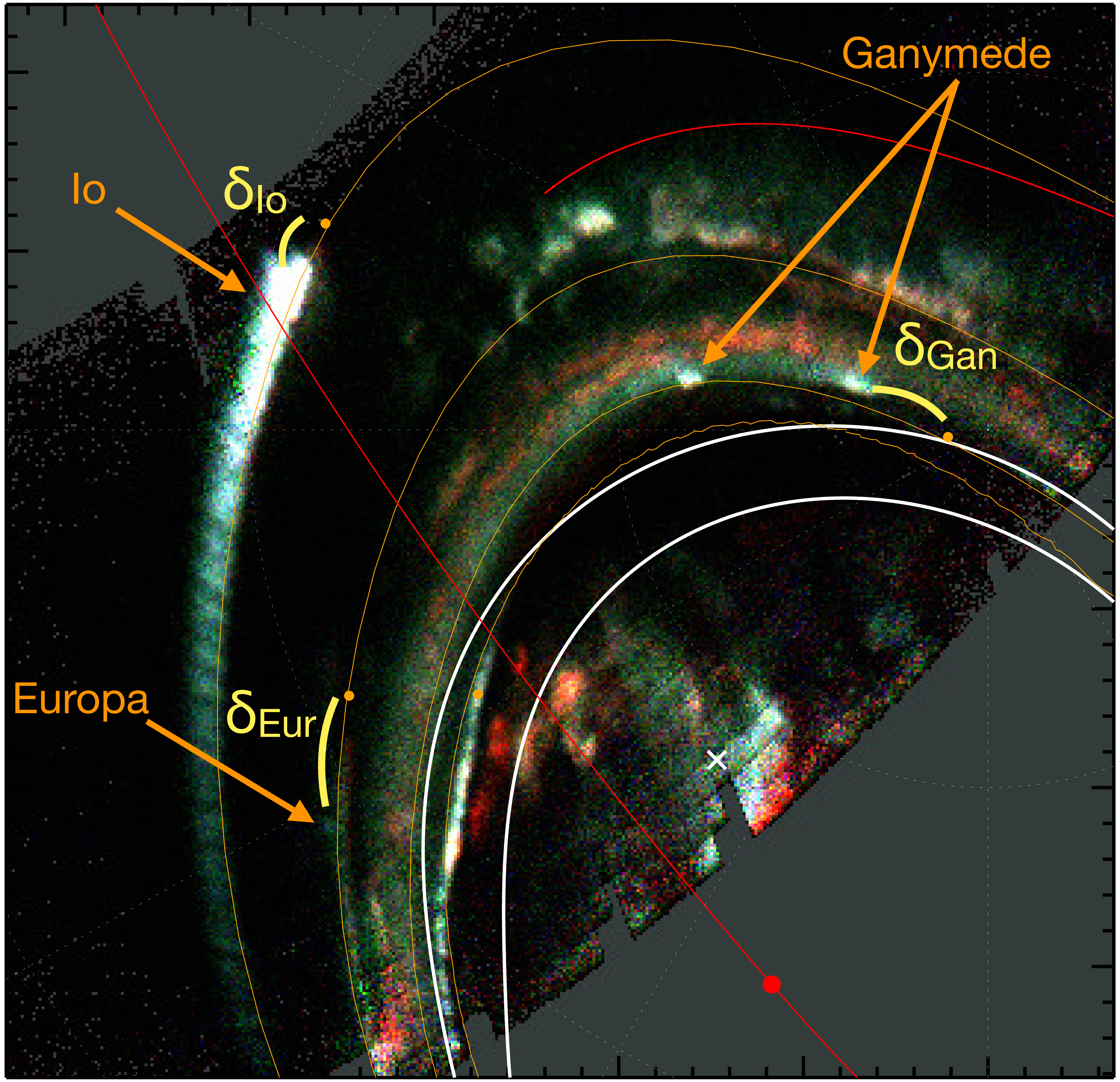

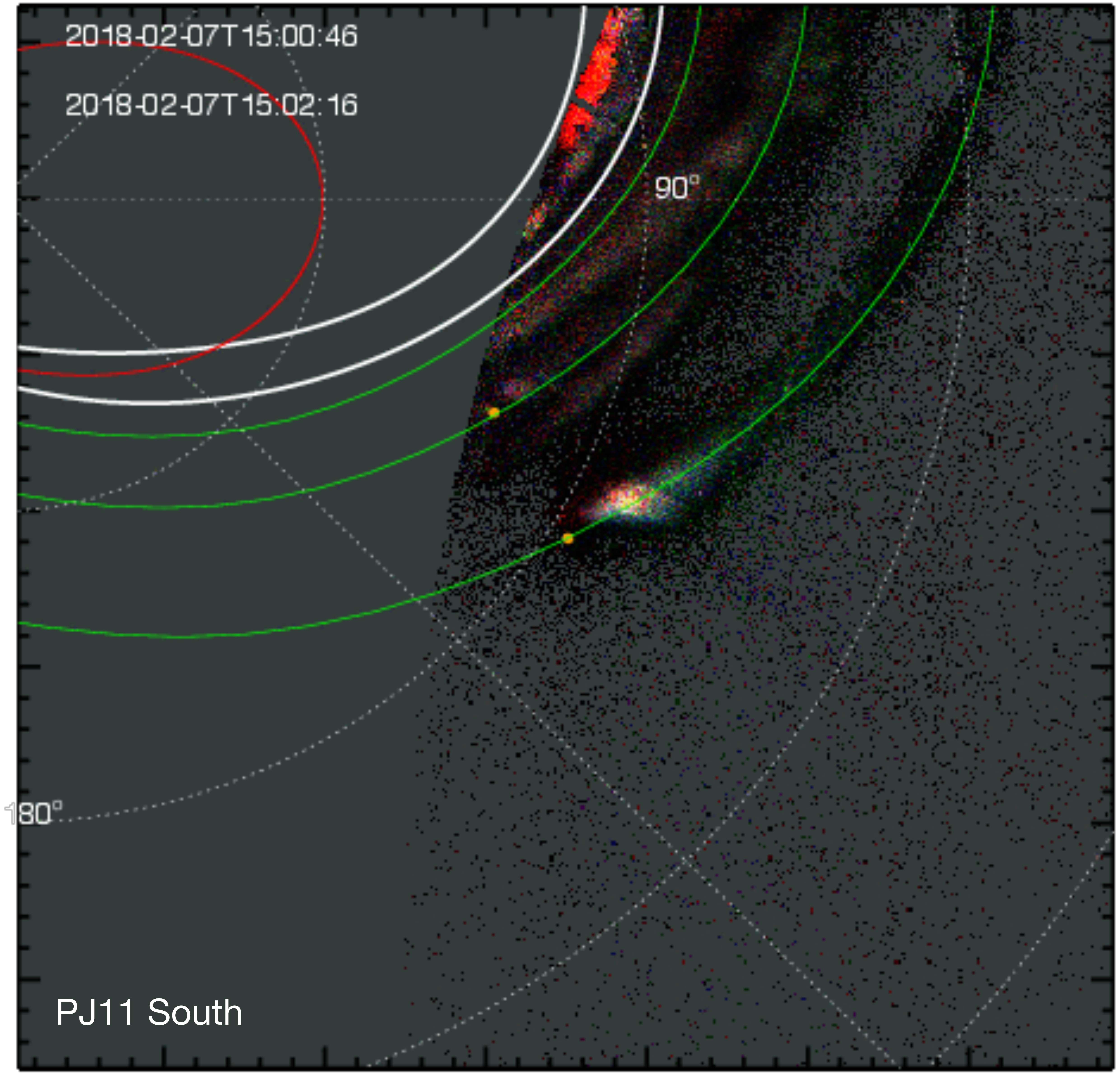

Juno-UVS
Data analysis

- 4-spin averaged data (2 min)
- Identification and hand selection of the MAW footprint
- Derivation of various parameters:
  - Distance to the reference contour
  - Emission angle
  - Error estimation

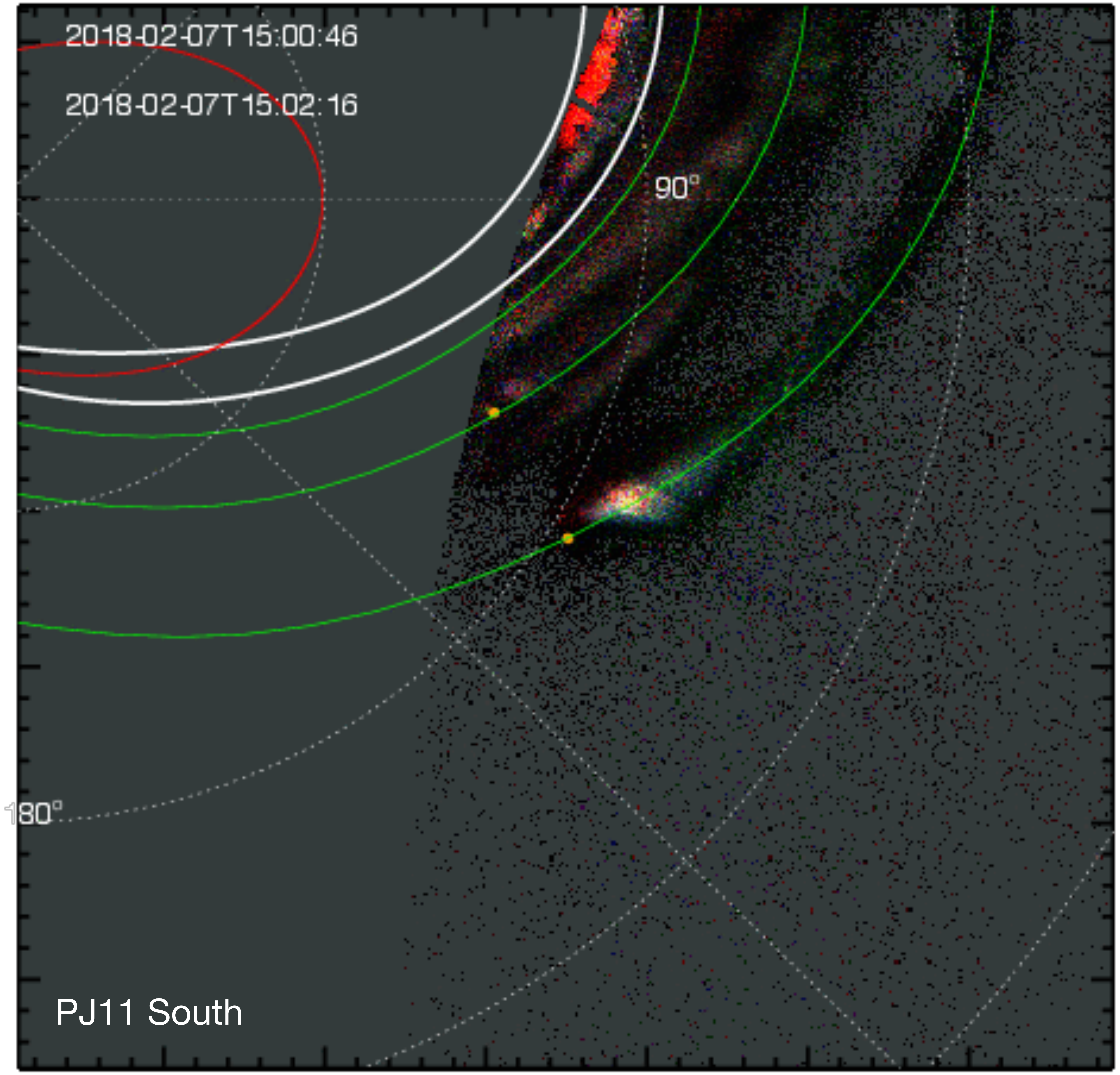

Juno-UVS
Data analysis

- 4-spin averaged data (2 min)
- Identification and hand selection of the MAW footprint
- Derivation of various parameters:
  - Distance to the reference contour
  - Emission angle
  - Error estimation

Southern hemisphere lead angle

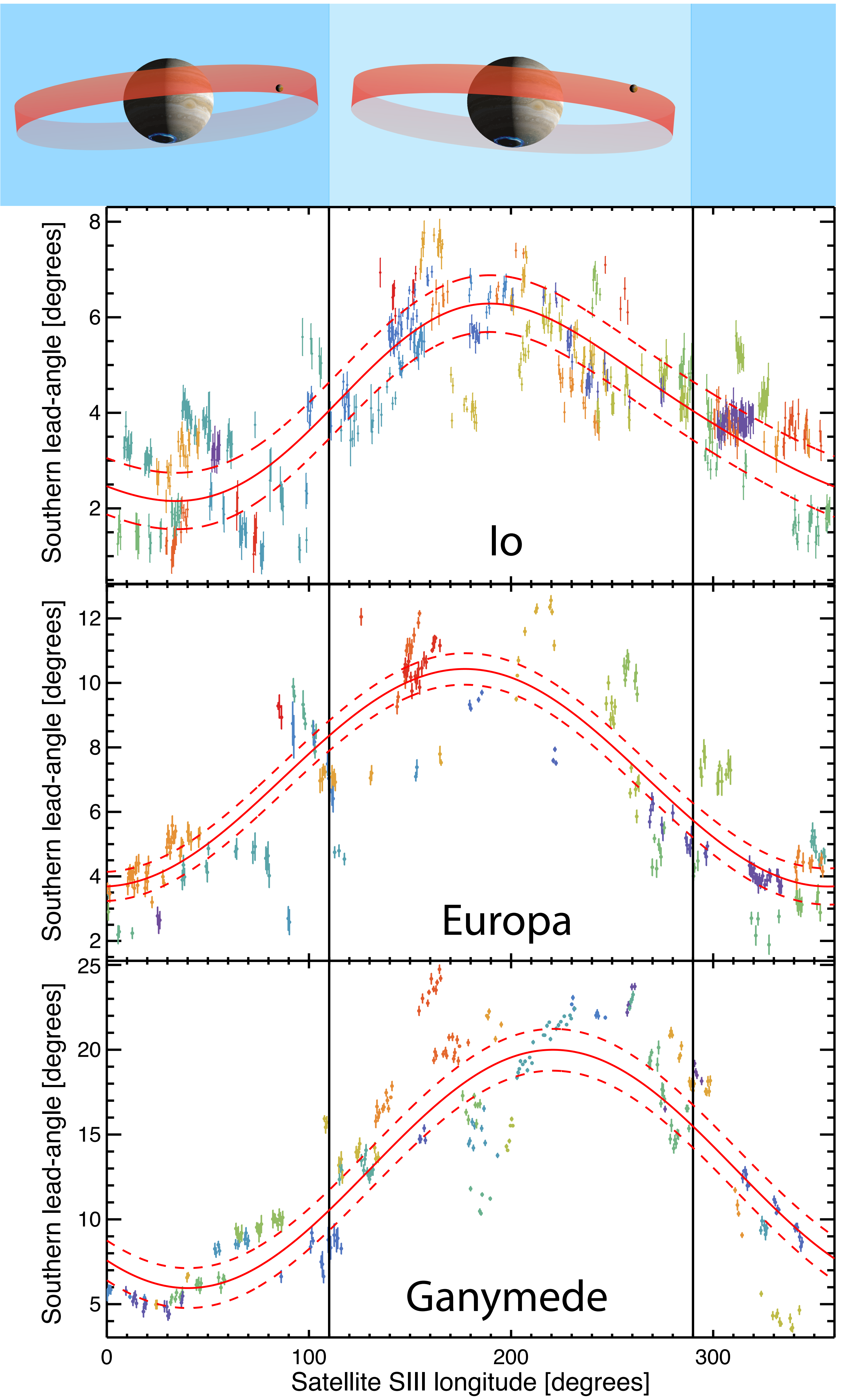

Hue+2023

Southern hemisphere lead angle

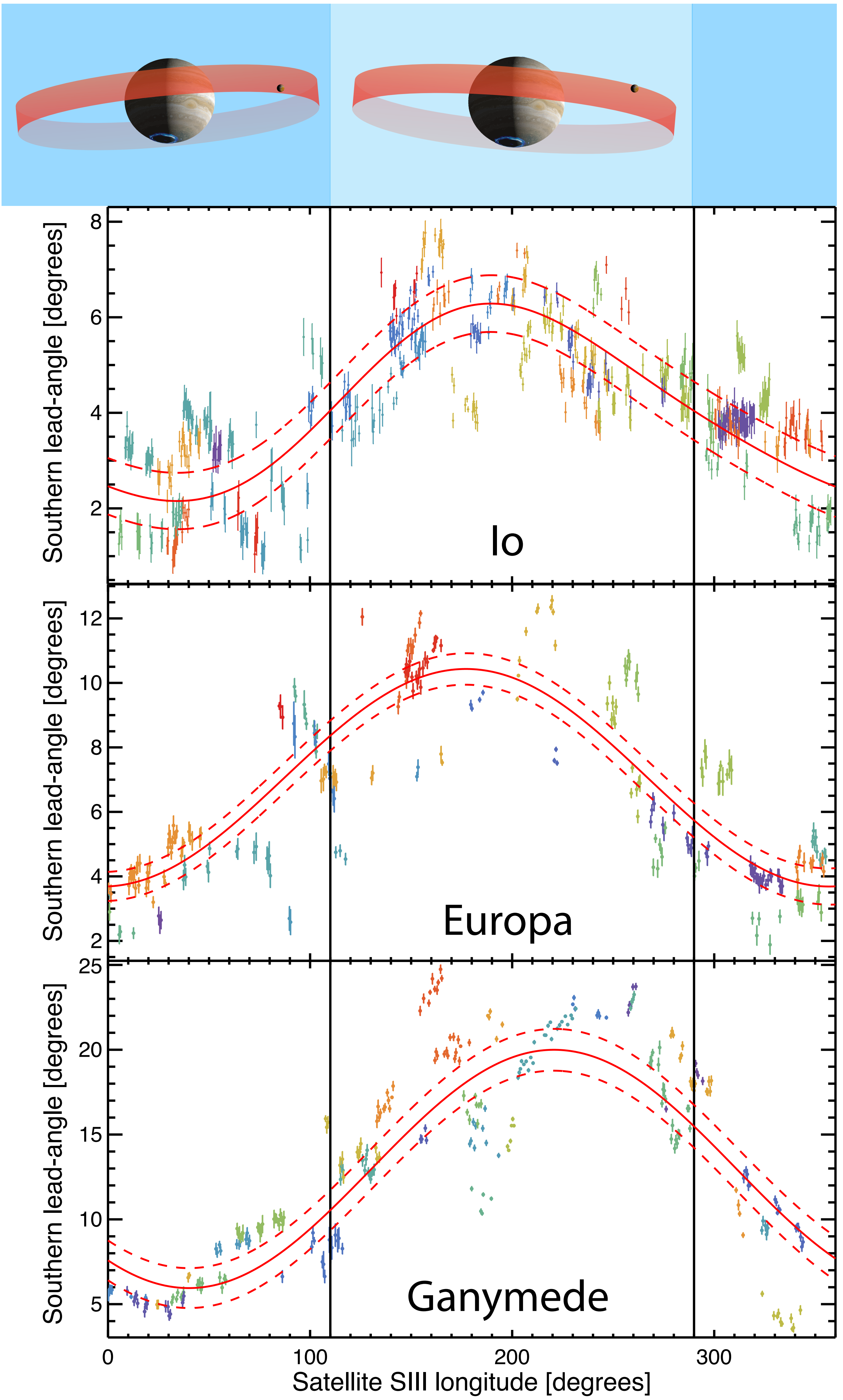

Hue+2023

$$t_A = \frac{P^{syn}_{moon} \times \delta_{moon}}{360},$$

Calculating Alfvén travel time from the lead angle and moon synodic periods

Southern hemisphere lead angle

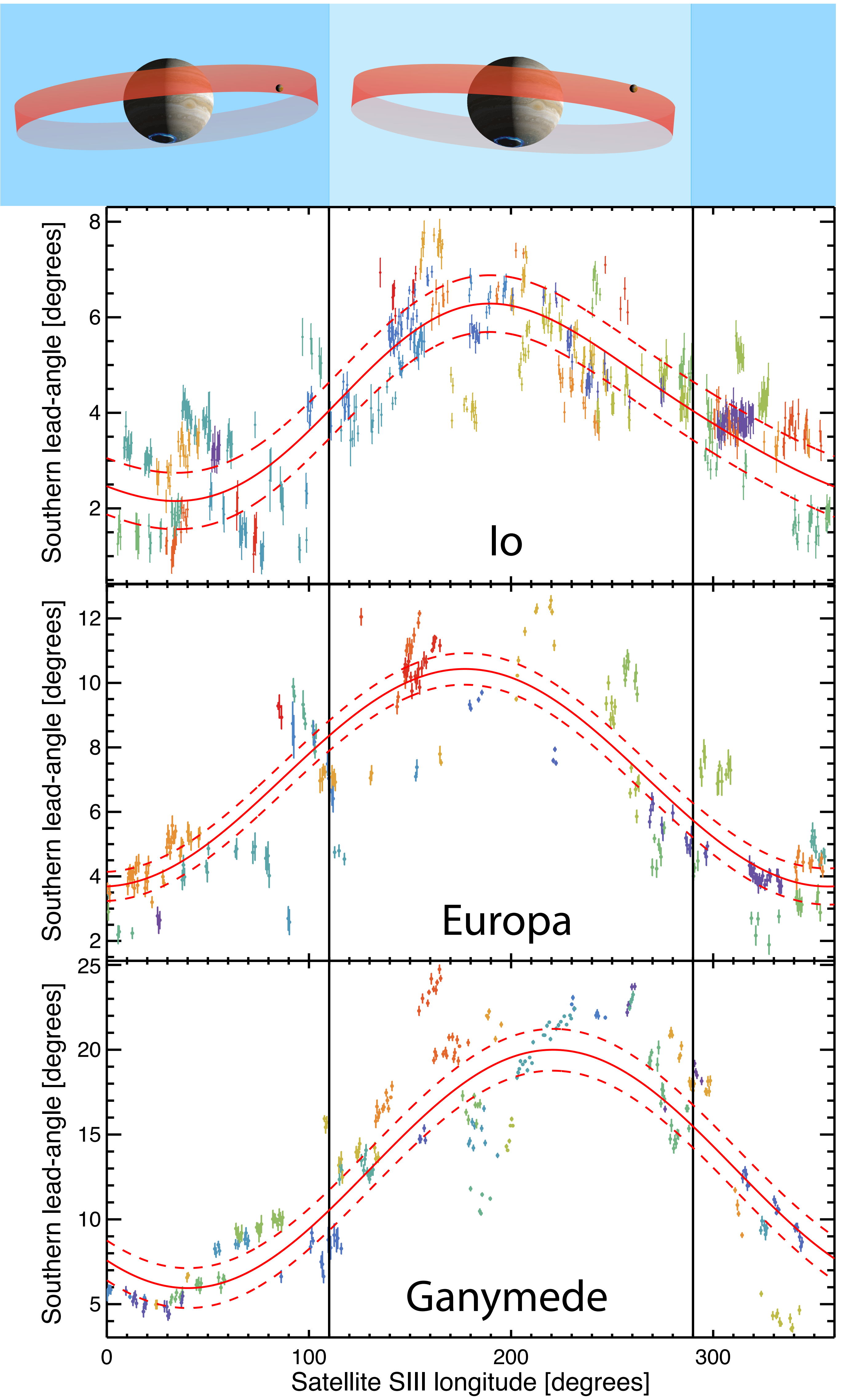

Hue+2023

$$t_A = \frac{P_{moon}^{syn} \times \delta_{moon}}{360},$$

Calculating Alfvén travel time from the lead angle and moon synodic periods

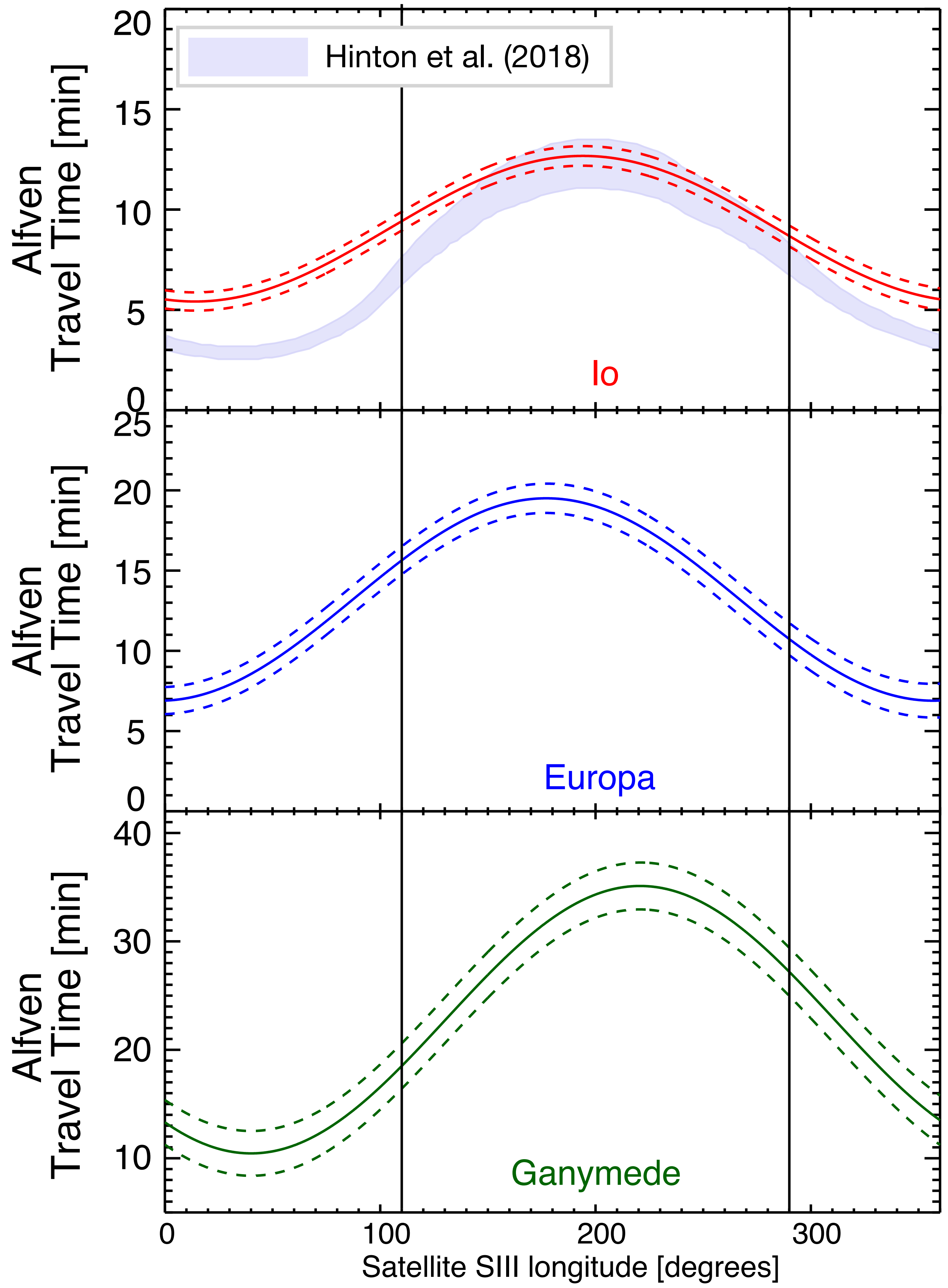

Fluxtube crossings at Io

Io

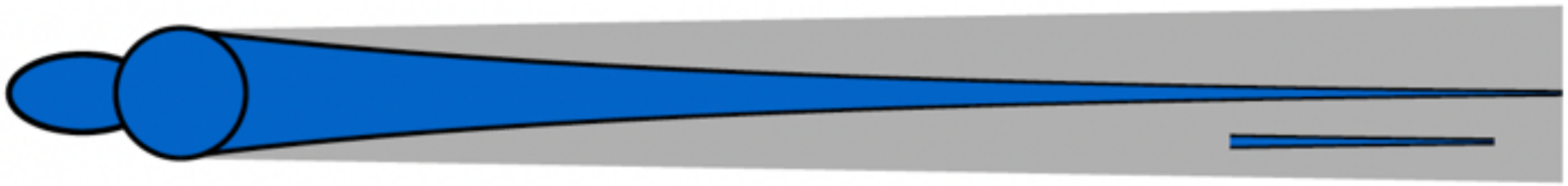

- Io MAW crossing (PJ12 N)
  - Broadband precipitating electrons EF
  - Poynting Flux ~1000 mW/m²
  - Alfvénic magnetic turbulence and whistler-mode waves
  - Proton acceleration (Clark+2020; Szalay+2020a; Szalay+2020c; Sulaiman+2020; Gershman+2019)
- Tail:
  - Broadband electron spectra with e-folding ~21°

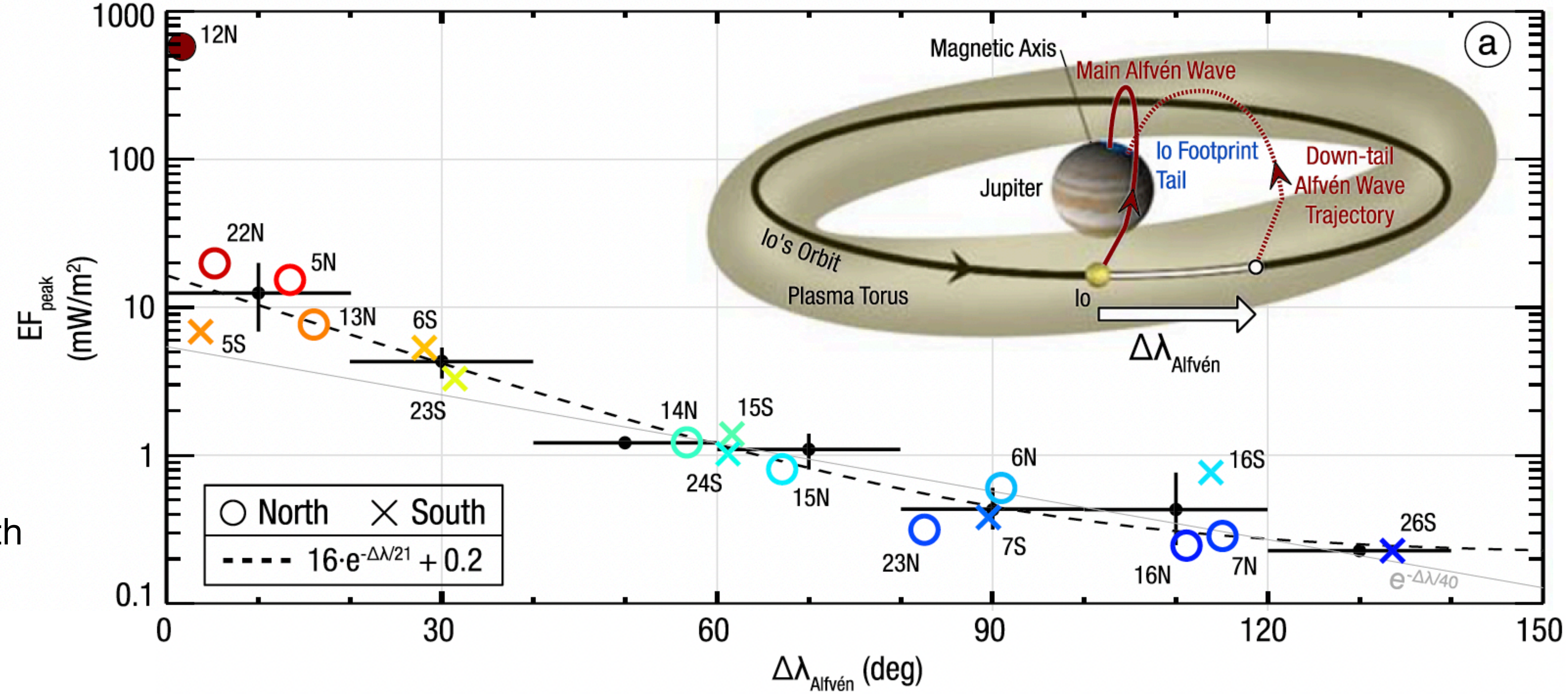

Szalay+2020c

Fluxtube crossings at Europa

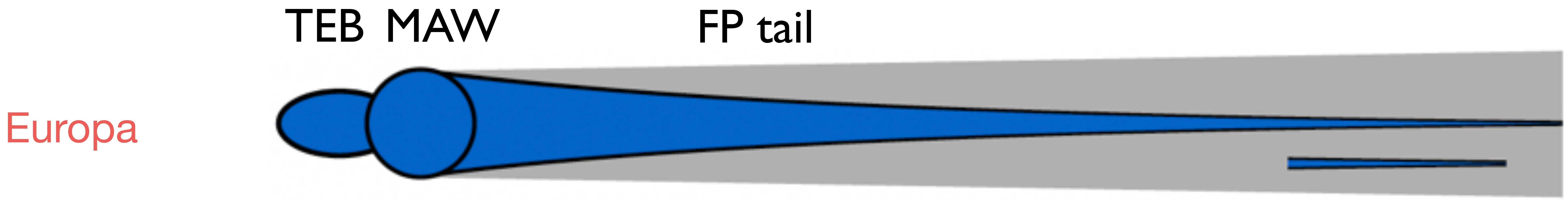

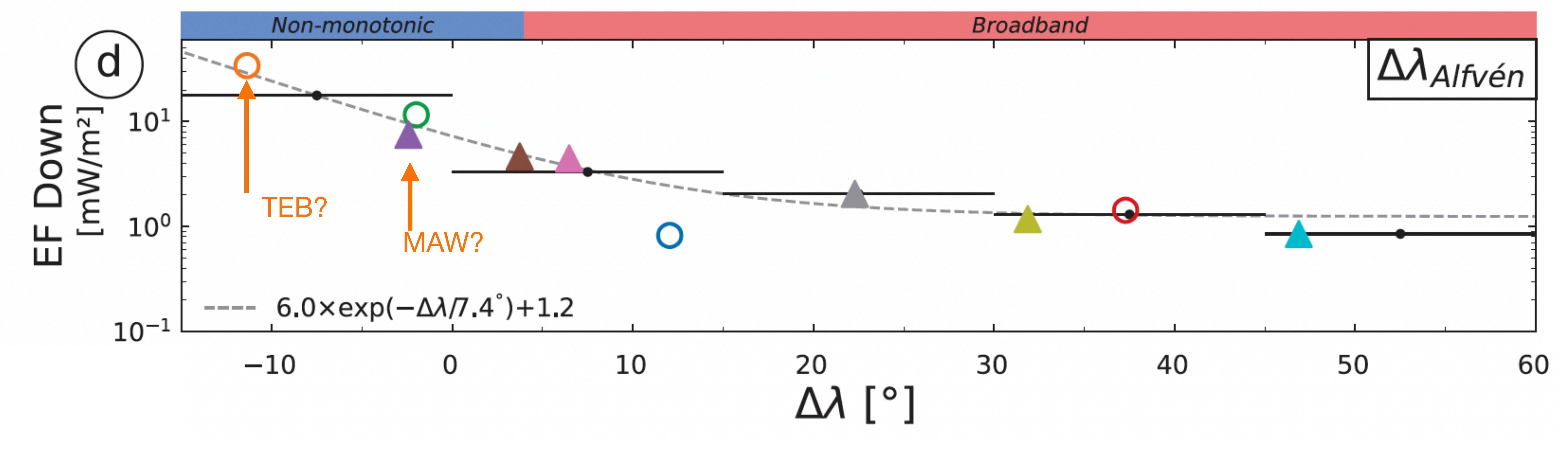

Rabia+2023

- Europa TEB crossing during PJ12N ? (Allegrini+2020)

- Near tail: non-monotonic electron distribution (Rabia+2023)
- Far tail: Broadband electron spectra with e-folding ~7.4°

Summary: Juno fluxtube crossings at Io, Eur., Gan.

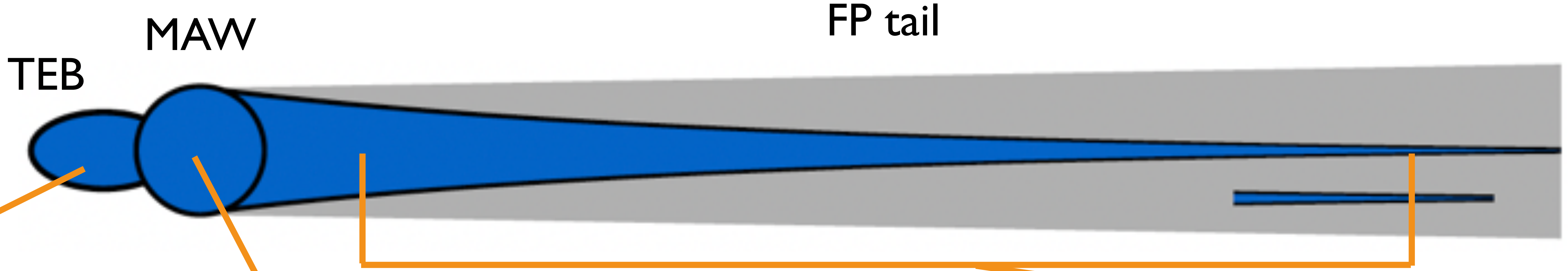

TEB crossings:

Io: **?**

Europa (PJ12N, Allegrini+2020)
➡Electrostatic e^- acceleration

Ganymede (PJ30S, Hue+2022)
➡Broadband e^- EF? Electrostatic e^- acceleration?
➡Poynting Flux: 3 mW/m^2
➡Down. e^- EF: 316 mW/m^2

➡Crossings survey: Rabia et al. in prep

MAW crossings:

Io (Gershman+2019; Clark+2020; Sulaiman+2020; Szalay+2020a,2020c)

➡Broadband e^- acceleration
➡Poynting Flux: 1000 mW/m^2
➡Down. e^- EF: 600 mW/m^2
➡Alfvénic magnetic turbulence and whistler-mode waves
➡Proton acceleration

Europa (Rabia+2023)
➡Electrostatic e^- acceleration (PJ13N, PJ23S)

Ganymede: **?**

Tail crossings:

Io (Szalay+2020c, Sulaiman+ 2023)
➡Broadband e^- EF
➡Down e- EF e-folding ~21˚
➡UV e-folding ~40˚
➡MAW efficiency ~10%

Europa (Rabia+2023)
➡Broadband e^- EF
➡Down e- EF e-folding ~7.4˚
➡UV e-folding ~21˚
➡Characteristic energy decreases downtail

Ganymede (PJ20S, Szalay+2020b, Louis+2020)
➡Broadband e^- EF
➡Crossings survey: Rabia et al. in prep

Summary: Juno fluxtube crossings at Io, Eur., Gan.

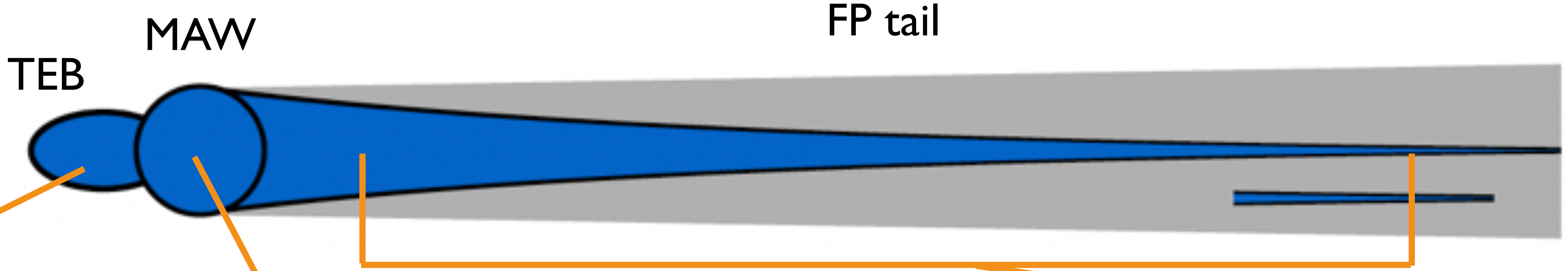

TEB crossings:

Io: **?**

Europa (PJ12N, Allegrini+2020)
➡Electrostatic e^- acceleration

Ganymede (PJ30S, Hue+2022)
➡Broadband e^- EF? Electrostatic e^- acceleration?
➡Poynting Flux: 3 mW/m^2
➡Down. e^- EF: 316 mW/m^2

➡Crossings survey: Rabia et al. in prep

MAW crossings:

Io (Gershman+2019; Clark+2020; Sulaiman+2020; Szalay+2020a,2020c)

➡Broadband e^- acceleration
➡Poynting Flux: 1000 mW/m^2
➡Down. e^- EF: 600 mW/m^2
➡Alfvénic magnetic turbulence and whistler-mode waves
➡Proton acceleration

Europa (Rabia+2023)
➡Electrostatic e^- acceleration (PJ13N, PJ23S)

Ganymede: **?**

Tail crossings:

Io (Szalay+2020c, Sulaiman+ 2023)
➡Broadband e^- EF
➡Down e- EF e-folding ~21˚
➡UV e-folding ~40˚
➡MAW efficiency ~10%

Europa (Rabia+2023)
➡Broadband e^- EF
➡Down e- EF e-folding ~7.4˚
➡UV e-folding ~21˚
➡Characteristic energy decreases downtail

Ganymede (PJ20S, Szalay+2020b, Louis+2020)
➡Broadband e^- EF
➡Crossings survey: Rabia et al. in prep

Check these posters out

59. Rabia, Jonas, et al., *Caractérisation in-situ des propriétés des électrons dans les circuits lunes-Jupiter et mécanismes d'accélération associés*
45. Louis, Corentin, *Source des émissions radio induites par les lunes galiléennes Io, Europa et Ganymède : mesures in situ par Juno*


Thank you!


Thank you!